

Policy Optimization with Stochastic Mirror Descent *

Long Yang¹, Yu Zhang², Gang Zheng¹, Qian Zheng³, Pengfei Li¹, Jianhang Huang¹, Jun Wen¹, and Gang Pan¹

¹College of Computer Science and Technology, Zhejiang University, China

²Netease Games AI Lab, HangZhou, China

³School of Electronics and Electrical Engineering, Nanyang Technological University, Singapore

¹{yanglong, gpan, gang_zheng, pfl, huangjianhang}@zju.edu.cn

²zhangyu15@corp.netease.com

³zhengqian@ntu.edu.sg

February 10, 2022

Abstract

Improving sample efficiency has been a longstanding goal in reinforcement learning. This paper proposes VRMPO algorithm: a sample efficient policy gradient method with stochastic mirror descent. In VRMPO, a novel variance-reduced policy gradient estimator is presented to improve sample efficiency. We prove that the proposed VRMPO needs only $\mathcal{O}(\epsilon^{-3})$ sample trajectories to achieve an ϵ -approximate first-order stationary point, which matches the best sample complexity for policy optimization. The extensive experimental results demonstrate that VRMPO outperforms the state-of-the-art policy gradient methods in various settings.

1 Introduction

Policy gradient [Williams, 1992; Sutton et al., 2000] is widely used to search the optimal policy in reinforcement learning (RL), and it has achieved significant successes in challenging fields such as playing Go [Silver et al., 2016, 2017] or robotics [Duan et al., 2016].

However, policy gradient methods suffer from high sample complexity, since many existing popular methods require to collect a lot of samples for each step to update its parameters [Mnih et al., 2016; Haarnoja et al., 2018; Meng et al., 2019; Xu et al., 2020; Xing et al., 2021], which partially reduces the effectiveness of the samples. Besides, it is still very challenging to provide a theoretical analysis of sample complexity for policy gradient methods instead of empirically improving sample efficiency.

To improve sample efficiency, this paper addresses how to design an efficient and convergent algorithm with stochastic mirror descent (SMD) [Nemirovsky and Yudin, 1983]. SMD keeps the advantage of low memory requirement and low computational complexity [Lei and Tang, 2018; Yang et al., 2021], which implies SMD needs less samples to learn a model. However, the significant challenges of applying the existing SMD to RL are two-fold: **1)** The objective of policy-based RL is a typical

*This submission has been accepted by AAAI 2022. L.Yang and Y.Zhang share an equal contribution for this work. L.Yang now is with Peking University, Email: yanglong001@pku.edu.cn. J. Wen is with Harvard Medical School, this work is done when he was at Zhejiang University, E-mail: jungel2star@gmail.com.

non-convex function, [Ghadimi et al., 2016] show that it may cause instability and even divergence when updating the parameter of a non-convex objective by SMD via a single sample. **2)** The large variance of policy gradient estimator is a critical bottleneck of improving sample efficiency for policy optimization with SMD. The non-stationary sampling process with the environment will lead to a large variance on the policy gradient estimator [Papini et al., 2018], which requires more samples to get a robust policy gradient and results in poor sample efficiency [Liu et al., 2018]. To address the above challenges:

We provide a theory analysis of the dilemma of applying SMD to policy optimization. Result (18) shows that under the Assumption 2.1, deriving the algorithm directly via SMD can not guarantee the convergence for policy optimization. Furthermore, we propose a new algorithm **MPO** that keeps a provable convergence guarantee (see Theorem 3.2). Designing a new gradient estimator according to historical information of policy gradient is the key to **MPO**.

We propose a variance-reduced mirror policy optimization algorithm (**VRMPO**): an efficient sample method via constructing a variance reduced policy gradient estimator. Concretely, we design an efficiently computable policy gradient estimator (see Eq.(26)) that utilizes fresh information and yields a more accurate estimation of the policy gradient, which is the key to improve sample efficiency. Theorem 4.1 illustrates that **VRMPO** needs $\mathcal{O}(\epsilon^{-3})$ sample trajectories to achieve an ϵ -approximate first-order stationary point (ϵ -FOSP). To our best knowledge, the proposed **VRMPO** matches the best sample complexity among the existing literature. Particularly, although **SRVR-PG** [Xu et al., 2020; Xu, 2021] achieves the same sample complexity as **VRMPO**, our approach needs less assumptions than [Xu et al., 2020; Xu, 2021], and our **VRMPO** unifies **SRVR-PG**. We have presented more comparisons and discussions in Remark 4.1. Besides, empirical result shows **VRMPO** converges faster than **SRVR-PG**.

2 Background and Stochastic Mirror Descent

Reinforcement learning (RL) is often formulated as *Markov decision processes* (MDP) $M = (\mathcal{S}, \mathcal{A}, P, R, \rho_0, \gamma)$, where \mathcal{S} is state space, \mathcal{A} is action space; $P(s'|s, a)$ is the probability of the state transition from s to s' under playing a ; $R(\cdot, \cdot) : \mathcal{S} \times \mathcal{A} \rightarrow [-R_{\max}, R_{\max}]$ is the reward function, where R_{\max} is a certain positive scalar. $\rho_0(\cdot) : \mathcal{S} \rightarrow [0, 1]$ is the initial state distribution and $\gamma \in (0, 1)$.

Policy $\pi_\theta(a|s)$ is a probability distribution on $\mathcal{S} \times \mathcal{A}$ with a parameter $\theta \in \mathbb{R}^p$. Let $\tau = \{s_t, a_t, r_{t+1}\}_{t=0}^{H_\tau}$ be a trajectory, where $s_0 \sim \rho_0(s_0)$, $a_t \sim \pi_\theta(\cdot|s_t)$, $r_{t+1} = R(s_t, a_t)$, $s_{t+1} \sim P(\cdot|s_t, a_t)$, and H_τ is the finite horizon of τ . The expected return function $J(\theta)$ is defined as follows,

$$J(\theta) \stackrel{\text{def}}{=} \int_{\tau} P(\tau|\theta) R(\tau) d\tau = \mathbb{E}_{\tau \sim \pi_\theta} [R(\tau)], \quad (1)$$

where $P(\tau|\theta) = \rho_0(s_0) \prod_{t=0}^{H_\tau} P(s_{t+1}|s_t, a_t) \pi_\theta(a_t|s_t)$ is the probability of generating τ , $R(\tau) = \sum_{t=0}^{H_\tau} \gamma^t r_{t+1}$ is the accumulated discounted return. Let $\mathcal{J}(\theta) = -J(\theta)$, the central problem of policy-based RL is to solve the problem:

$$\theta^* = \arg \max_{\theta} J(\theta) \iff \theta^* = \arg \min_{\theta} \mathcal{J}(\theta). \quad (2)$$

Computing $\nabla J(\theta)$ analytically, we have

$$\nabla J(\theta) = \mathbb{E}_{\tau \sim \pi_\theta} \left[\sum_{t \geq 0} \nabla_{\theta} \log \pi_{\theta}(a_t|s_t) R(\tau) \right]. \quad (3)$$

Let $g(\tau|\theta) = \sum_{t=0}^{H_\tau} \nabla_{\theta} \log \pi_{\theta}(a_t|s_t) R(\tau)$, which is an unbiased estimator of $\nabla J(\theta)$. Vanilla policy gradient (VPG) is a straightforward way to solve problem (2) as follows,

$$\theta \leftarrow \theta + \alpha g(\tau|\theta),$$

where α is step size.

Assumption 2.1. [Papini et al., 2018] *For each pair $(s, a) \in \mathcal{S} \times \mathcal{A}$, $\theta \in \mathbb{R}^p$, and all components i, j , there exists positive constants G, F such that:*

$$|\nabla_{\theta_i} \log \pi_{\theta}(a|s)| \leq G, \quad \left| \frac{\partial^2}{\partial \theta_i \partial \theta_j} \log \pi_{\theta}(a|s) \right| \leq F. \quad (4)$$

Assumption 2.1 implies $\nabla J(\theta)$ is L -Lipschitz [Papini et al., 2018, Lemma B.2], i.e.,

$$\|\nabla J(\theta_1) - \nabla J(\theta_2)\| \leq L \|\theta_1 - \theta_2\|, \quad (5)$$

where $L = R_{\max} H_{\tau} (H_{\tau} G^2 + F) / (1 - \gamma)$. Besides, under Assumption 2.1, Shen et al. [2019] have shown the property:

$$\|g(\tau|\theta) - \nabla J(\theta)\|_2^2 \leq \frac{G^2 R_{\max}^2}{(1 - \gamma)^4} =: \sigma^2. \quad (6)$$

2.1 SMD and Bregman Gradient

Now, we review some basic concepts of stochastic mirror descent(SMD) and Bregman gradient.

Let's consider the stochastic optimization problem,

$$\min_{\theta \in D_{\theta}} \{f(\theta) = \mathbb{E}[F(\theta; \xi)]\}, \quad (7)$$

where $D_{\theta} \in \mathbb{R}^n$ is a nonempty convex compact set, ξ is a random vector whose probability distribution μ is supported on $\Xi \in \mathbb{R}^d$ and $F : D_{\theta} \times \Xi \rightarrow \mathbb{R}$. We assume that the expectation $\mathbb{E}[F(\theta; \xi)] = \int_{\Xi} F(\theta; \xi) d\mu(\xi)$ is well defined and finite-valued for every $\theta \in D_{\theta}$.

Definition 2.1 (Proximal Operator). *Let T be defined on a closed convex \mathcal{X} , and $\alpha > 0$. The proximal operator of T is*

$$\mathcal{M}_{\alpha, T}^{\psi}(z) = \arg \min_{x \in \mathcal{X}} \left\{ T(x) + \frac{1}{\alpha} D_{\psi}(x, z) \right\}, \quad (8)$$

where $\psi(\cdot)$ is a continuously-differentiable, ζ -strictly convex function satisfies $\langle x - y, \nabla \psi(x) - \nabla \psi(y) \rangle \geq \zeta \|x - y\|^2, \zeta > 0$, $D_{\psi}(\cdot, \cdot)$ is Bregman distance: $\forall x, y \in \mathcal{X}$,

$$D_{\psi}(x, y) = \psi(x) - \psi(y) - \langle \nabla \psi(y), x - y \rangle.$$

Stochastic Mirror Descent (SMD). The SMD solves (7) by generating an iterative solution as follows,

$$\theta_{t+1} = \mathcal{M}_{\alpha_t, \ell(\theta)}^{\psi}(\theta_t) = \arg \min_{\theta \in D_{\theta}} \left\{ \langle g_t, \theta \rangle + \frac{1}{\alpha_t} D_{\psi}(\theta, \theta_t) \right\}, \quad (9)$$

where $\alpha_t > 0$ is step-size, $\ell(\theta) = \langle g_t, \theta \rangle$ is the first-order approximation of $f(\theta)$ at θ_t , $g_t = g(\theta_t, \xi_t)$ is stochastic subgradient such that $g(\theta_t) = \mathbb{E}[g(\theta_t, \xi_t)] \in \partial f(\theta)|_{\theta=\theta_t}$, $\{\xi_t\}_{t \geq 0}$ represents a draw from distribution μ , and $\partial f(\theta) = \{g | f(\theta) - f(\omega) \leq g^\top(\theta - \omega), \forall \omega \in \text{dom}(f)\}$. If we choose $\psi(x) = \frac{1}{2}\|x\|_2^2$, then $D_\psi(x, y) = \frac{1}{2}\|x - y\|_2^2$, since then iteration (9) is reduced to stochastic gradient decent (SGD).

Convergence Criteria: Bregman Gradient. Recall \mathcal{X} is a closed convex set on \mathbb{R}^n , $\alpha > 0$, $T(x)$ is defined on \mathcal{X} . The Bregman gradient of T at $x \in \mathcal{X}$ is defined as:

$$\mathcal{G}_{\alpha, T}^\psi(x) = \alpha^{-1}(x - \mathcal{M}_{\alpha, T}^\psi(x)), \quad (10)$$

where $\mathcal{M}_{\alpha, T}^\psi(\cdot)$ is defined in Eq.(8). If $\psi(x) = \frac{1}{2}\|x\|_2^2$, according to [Bauschke et al., 2011, Theorem 27.1], then x^* is a critical point of T if and only if $\mathcal{G}_{\alpha, T}^\psi(x^*) = \nabla T(x^*) = 0$. Thus, Bregman gradient (10) is a generalization of standard gradient. Remark 2.1 provides us some insights to understand Bregman gradient as a convergence criterion.

Remark 2.1. Let $T(\cdot)$ be a convex function, according to [Bertsekas, 2009, Proposition 5.4.7]: x^* is a stationarity point of $T(\cdot)$ if and only if

$$0 \in \partial(T + \delta_{\mathcal{X}})(x^*), \quad (11)$$

where $\delta_{\mathcal{X}}(\cdot)$ is the indicator function on \mathcal{X} . Furthermore, if $\psi(x)$ is twice continuously differentiable, let $\tilde{x} = \mathcal{M}_{\alpha, T}^\psi(x)$, by the definition of $\mathcal{M}_{\alpha, T}^\psi(\cdot)$ (8), we have

$$0 \in \partial(T + \delta_{\mathcal{X}})(\tilde{x}) + (\nabla\psi(\tilde{x}) - \nabla\psi(x)) \stackrel{(*)}{\approx} \partial(T + \delta_{\mathcal{X}})(\tilde{x}) + \alpha\mathcal{G}_{\alpha, T}^\psi(x)\nabla^2\psi(x), \quad (12)$$

Eq.(*) holds due to Taylor expansion of $\nabla\psi(x)$ on first order. If $\mathcal{G}_{\alpha, T}^\psi(x) \approx 0$, Eq.(12) implies the origin point 0 is near the set $\partial(T + \delta_{\mathcal{X}})(\tilde{x})$, i.e., according to the criteria (11), \tilde{x} is close to a stationary point. For the iteration (9), we focus on the time when it makes the $\mathcal{G}_{\alpha, T}^\psi(\theta_t)$ near origin point $\mathbf{0}$. Formally, we are satisfied with finding an ϵ -approximate first-order stationary point (ϵ -FOSP) θ_ϵ such that

$$\|\mathcal{G}_{\alpha, T}^\psi(\theta_\epsilon)\|_2 \leq \epsilon. \quad (13)$$

Particularly, for policy optimization (2), we would choose $T(\theta) = \langle -\nabla J(\theta), \theta \rangle$.

3 Stochastic Mirror Policy Optimization

In this section, we solve the problem (2) via SMD. Firstly, we analyze the theoretical dilemma of applying SMD directly to policy optimization, and result shows that under the common Assumption 2.1, there still lacks a provable guarantee of solving (2) via SMD directly. Then, we propose a convergent mirror policy optimization algorithm (MPO).

3.1 Theoretical Dilemma

For each $k \in [1, N - 1]$, $\tau_k = \{s_t, a_t, r_{t+1}\}_{t=0}^{H_{\tau_k}} \sim \pi_{\theta_k}$, and we receive the gradient information as follows,

$$-g(\tau_k|\theta_k) = -\sum_{t \geq 0} \nabla_\theta \log \pi_\theta(a_t|s_t) R(\tau_k)|_{\theta=\theta_k}. \quad (14)$$

According to (9), we define the update rule as follows,

$$\theta_{k+1} = \mathcal{M}_{\alpha_k, \langle -g(\tau_k|\theta_k), \theta \rangle}^\psi(\theta_k) = \arg \min_{\theta} \left\{ \langle -g(\tau_k|\theta_k), \theta \rangle + \frac{1}{\alpha_k} D_\psi(\theta, \theta_k) \right\}, \quad (15)$$

where α_k is step-size. After $(N - 1)$ episodes, we receive a collection $\{\theta_k\}_{k=1}^N$. Since $-J(\theta)$ is non-convex, according to Ghadimi, et al [Ghadimi et al., 2016], a standard strategy for analyzing non-convex optimization is to pick up the output $\tilde{\theta}_N$ from the following distribution (16) over $\{1, 2, \dots, N\}$:

$$\mathbb{P}(\tilde{\theta}_N = \theta_k) = \frac{\zeta \alpha_k - L \alpha_k^2}{\sum_{i=1}^N (\zeta \alpha_i - L \alpha_i^2)}, k \in [1, N], \quad (16)$$

where step-size $\alpha_k \in (0, \zeta/L)$.

Theorem 3.1. [Ghadimi et al., 2016] *Under Assumption 2.1, consider the sequence $\{\theta_k\}_{k=1}^N$ generated by (15), the output $\tilde{\theta}_N = \theta_k$ follows the distribution (16). Let $\ell(g, u) = \langle g, u \rangle$, $g_k = (\tau_k|\theta_k)$, Let $\Delta = J(\theta^*) - J(\theta_1)$. Then,*

$$\mathbb{E} \left[\left\| \mathcal{G}_{\alpha_k, \ell(-g_k, \theta_k)}^\psi(\tilde{\theta}_N) \right\|_2^2 \right] \leq \frac{\Delta + \sigma^2 / \zeta \sum_{i=1}^N \alpha_i}{\sum_{i=1}^N (\zeta \alpha_i - L \alpha_i^2)}. \quad (17)$$

Unfortunately, the lower bound of (17) reaches

$$\frac{J(\theta^*) - J(\theta_1) + \sigma^2 / \zeta \sum_{i=1}^N \alpha_i}{\sum_{i=1}^N (\zeta \alpha_i - L \alpha_i^2)} \geq \frac{\sigma^2}{\zeta^2}, \quad (18)$$

which can not guarantee the convergence of (15), no matter how the step-size α_k is specified. Thus, under Assumption 2.1, updating parameters according to (15) and the output following (16) lacks a provable convergence guarantee.

Discussion 1 (Open Problems). *Eq.(15) is a general rule that unifies many existing algorithms. If $\psi(\theta) = \frac{1}{2} \|\theta\|_2^2$, then (15) is VPG Williams [1992]. The update (15) is natural policy gradient Kakade [2002] if we choose $\psi(\theta) = \frac{1}{2} \theta^\top F(\theta) \theta$, where $F(\theta) = \mathbb{E}_{\tau \sim \pi_\theta} [\nabla_\theta \log \pi_\theta(s, a) \nabla_\theta \log \pi_\theta(s, a)^\top]$ is Fisher information matrix. If ψ is Boltzmann-Shannon entropy, then D_ψ is KL divergence and update (15) is reduced to relative entropy policy search [Peters et al., 2010; Tomar et al., 2020]. Despite extensive works around above methods, existing works are scattered and fragmented in both theoretical and empirical aspects [Agarwal et al., 2020]. Thus, it is of great significance to establish the fundamental theoretical convergence properties of iteration (15):*

What conditions guarantee the convergence of (15)?

This is an open problem. From the previous discussion, intuitively, the iteration (15) is a convergent scheme since particular mirror maps ψ can lead (15) to some popular empirically effective policy-based RL algorithms, but there still lacks a complete theoretical convergence analysis of (15).

3.2 MPO: A Convergent Implementation

In this section, we propose a convergent mirror policy optimization (MPO) as follows, for each step k :

$$\theta_{k+1} = \mathcal{M}_{\alpha_k, \langle -\hat{g}_k, \theta \rangle}^\psi(\theta_k) = \arg \min_{\theta \in \Theta} \left\{ \langle -\hat{g}_k, \theta \rangle + \frac{1}{\alpha_k} D_\psi(\theta, \theta_k) \right\}, \quad (19)$$

Algorithm 1 MPO

- 1: **Initialize:** parameter θ_1 , step-size $\alpha_k > 0$, $g_0 = 0$, parametric policy $\pi_\theta(a|s)$, and map ψ .
- 2: **for** $k = 1$ **to** N **do**
- 3: Generate a trajectory $\tau_k = \{s_t, a_t, r_{t+1}\}_{t=0}^{H_{\tau_k}} \sim \pi_{\theta_k}$, temporary variable $g_0 = 0$.

$$g_k \leftarrow \sum_{t=0}^{H_{\tau_k}} \nabla_\theta \log \pi_\theta(a_t|s_t) R(\tau_k)|_{\theta=\theta_k} \quad (21)$$

$$\hat{g}_k \leftarrow \frac{1}{k} g_k + \left(1 - \frac{1}{k}\right) \hat{g}_{k-1} \quad (22)$$

$$\theta_{k+1} \leftarrow \arg \min_{\omega} \left\{ \langle -\hat{g}_k, \omega \rangle + \frac{1}{\alpha_k} D_\psi(\omega, \theta_k) \right\} \quad (23)$$

4: **end for**

5: **Output** $\tilde{\theta}_N$ according to (16).

where \hat{g}_k is an arithmetic mean of previous episodes' gradient estimate $\{g(\tau_i|\theta_i)\}_{i=1}^k$:

$$\hat{g}_k = \frac{1}{k} \sum_{i=1}^k g(\tau_i|\theta_i). \quad (20)$$

We present the details of an implementation of MPO in Algorithm 1. Eq.(22) is an incremental implementation of the average (20), thus, (22) enjoys a lower storage cost than (20).

For a given episode, the gradient flow (20)/(22) of MPO is slightly different from the traditional VPG, REINFORCE [Williams, 1992], or DPG [Silver et al., 2014] whose gradient estimator (14) follows the current episode, while our MPO uses an arithmetic mean of all the previous policy gradients. The gradient estimator (14) is a natural way to estimate the term

$$-\nabla J(\theta_t) = -\mathbb{E} \left[\sum_{k=0}^{H_{\tau_t}} \nabla_\theta \log \pi_\theta(a_k|s_k) R(\tau_t) \right],$$

i.e., using the current trajectory to estimate policy gradient. Unfortunately, under Assumption 2.1, the result of (18) shows using (14) with SMD lacks a guarantee of convergence. This is exactly the reason why we abandon the way (14) and turn to propose (20)/(22) to estimate policy gradient.

Theorem 3.2 (Convergence of Algorithm 1). *Under Assumption 2.1, and the total trajectories are $\{\tau_k\}_{k=1}^N$. Consider the sequence $\{\theta_k\}_{k=1}^N$ generated by Algorithm 1, and the output $\tilde{\theta}_N = \theta_n$ follows the distribution of (16). Let $0 < \alpha_k < \frac{\zeta}{L}$, $\ell(g, u) = \langle g, u \rangle$, $\hat{g}_k = \frac{1}{k} \sum_{i=1}^k g_i$, and $\Delta = J(\theta^*) - J(\theta_1)$, where $g_i = \sum_{t=0}^{H_{\tau_i}} \nabla_\theta \log \pi_\theta(a_t|s_t) R(\tau_i)|_{\theta=\theta_i}$. Then the output $\tilde{\theta}_N = \theta_n$ satisfies*

$$\mathbb{E} \left[\|\mathcal{G}_{\alpha_n, \ell(-g_n, \theta_n)}^\psi(\theta_n)\|_2^2 \right] \leq \frac{\Delta + \sigma^2 / \zeta \sum_{k=1}^N \frac{\alpha_k}{k}}{\sum_{k=1}^N (\zeta \alpha_k - L \alpha_k^2)}. \quad (24)$$

For the proof, see Appendix B.

Let $\alpha_k = \frac{\zeta}{2L}$, then

$$\mathbb{E} \left[\|\mathcal{G}_{\alpha_n, \ell(-\hat{g}_n, \theta_n)}^\psi(\theta_n)\|_2^2 \right] \leq \frac{4L\Delta + 2\sigma^2 \sum_{k=1}^N \frac{1}{k}}{N\zeta^2} = \mathcal{O} \left(\frac{\ln N}{N} \right).$$

Our scheme of MPO partially answers the previous open problem through conducting a new policy gradient.

4 VRMPO: Variance Reduction Mirror Policy Optimization

In this section, we propose a variance reduction version of MPO: VRMPO. Inspired by the above work of Nguyen et al. [017a], we provide an efficiently computable policy gradient estimator; then, we prove that the VRMPO needs $\mathcal{O}(\epsilon^{-3})$ sample trajectories to achieve an ϵ -FOSP that matches the best sample complexity.

4.1 Methodology

For any initial θ_0 , let $\{\tau_j^0\}_{j=1}^N \sim \pi_{\theta_0}$, we estimate the initial policy gradient as follows,

$$G_0 = -\hat{\nabla}_N J(\theta_0) \stackrel{\text{def}}{=} -\frac{1}{N} \sum_{j=1}^N g(\tau_j^0 | \theta_0). \quad (25)$$

Let $\theta_1 = \theta_0 - \alpha G_0$, for each step $k \in \mathbb{N}^+$, let $\{\tau_j^k\}_{j=1}^N$ be the trajectories generated by π_{θ_k} , we define the policy gradient estimator G_k and update rule as follows,

$$G_k = G_{k-1} + \frac{1}{N} \sum_{j=1}^N \left(-g(\tau_j^k | \theta_k) + g(\tau_j^k | \theta_{k-1}) \right), \quad (26)$$

$$\theta_{k+1} = \arg \min_{\theta} \left\{ \langle G_k, \theta \rangle + \frac{1}{\alpha} D_{\psi}(\theta, \theta_k) \right\}. \quad (27)$$

In (26), $-g(\tau_j^k | \theta_k)$ and $g(\tau_j^k | \theta_{k-1})$ share the same trajectory $\{\tau_j^k\}_{j=1}^N$, which plays a critical role in reducing the variance of gradient estimator [Shen et al., 2019]. Besides, it is different from (20), we admit a simple recursive formulation to conduct the gradient estimator, see (26), which captures the technique from SARAH [Nguyen et al., 017a]. For each step k , the term

$$\frac{1}{N} \sum_{j=1}^N \left(-g(\tau_j^k | \theta_k) + g(\tau_j^k | \theta_{k-1}) \right)$$

can be seen as an additional ‘‘noise’’ for the policy gradient estimate. A lot of practices show that conducting a gradient estimator with such additional ‘‘noise’’ enjoys a lower variance and speeding up the convergence [Reddi et al., 2016]. More details are shown in Algorithm 2.

Theorem 4.1 (Convergence Analysis). *Consider $\{\tilde{\theta}_k\}_{k=1}^K$ generated by Algorithm 2. Under Assumption 2.1, and let $\zeta > \frac{5}{32}$. For any positive scalar ϵ , let batch size of the trajectories of the outer loop*

$$N_1 = \left(\frac{1}{8L\zeta^2} + \frac{1}{2(\zeta - \frac{5}{32})} \left(1 + \frac{1}{32\zeta^2} \right) \right) \frac{\sigma^2}{\epsilon^2},$$

$$m - 1 = N_2 = \sqrt{\left(\frac{1}{8L\zeta^2} + \frac{1}{2(\zeta - \frac{5}{32})} \left(1 + \frac{1}{32\zeta^2} \right) \right) \frac{\sigma}{\epsilon}},$$

Algorithm 2 VRMPO.

- 1: **Initialize:** Policy $\pi_\theta(a|s)$ with parameter $\tilde{\theta}_0$, mirror map ψ , step-size $\alpha > 0$, epoch size K, m .
- 2: **for** $k = 1$ **to** K **do**
- 3: $\theta_{k,0} = \tilde{\theta}_{k-1}$, generate $\mathcal{T}_k = \{\tau_i\}_{i=1}^{N_1} \sim \pi_{\theta_{k,0}}$
- 4: $\theta_{k,1} = \theta_{k,0} - \alpha G_{k,0}$, where $G_{k,0} = -\hat{\nabla}_{N_1} J(\theta_{k,0}) = -\frac{1}{N_1} \sum_{i=1}^{N_1} g(\tau_i|\theta_{k,0})$.
- 5: **for** $t = 1$ **to** $m - 1$ **do**
- 6: Generate $\{\tau_j\}_{j=1}^{N_2} \sim \pi_{\theta_{k,t}}$

$$G_{k,t} = G_{k,t-1} + \frac{1}{N_2} \sum_{j=1}^{N_2} (-g(\tau_j|\theta_{k,t}) + g(\tau_j|\theta_{k,t-1})), \quad (28)$$

$$\theta_{k,t+1} = \arg \min_{\omega} \left\{ \langle G_{k,t}, \omega \rangle + \frac{1}{\alpha} D_\psi(\omega, \theta_{k,t}) \right\}. \quad (29)$$

- 7: **end for**
 - 8: $\tilde{\theta}_k = \theta_{k,t}$ with t chosen uniformly randomly from $\{0, 1, \dots, m\}$.
 - 9: **end for**
 - 10: **Output:** $\tilde{\theta}_K$.
-

the outer loop times

$$K = \frac{8L(\mathbb{E}[\mathcal{J}(\tilde{\theta}_0)] - \mathcal{J}(\theta^*)) \left(1 + \frac{1}{16\zeta^2}\right) \frac{\sigma}{\epsilon}}{\sqrt{\left(\frac{1}{8L\zeta^2} + \frac{1}{2(\zeta - \frac{5}{32})} \left(1 + \frac{1}{32\zeta^2}\right) \left(\zeta - \frac{5}{32}\right)\right) \frac{\sigma}{\epsilon}}},$$

and step size $\alpha = \frac{1}{4L}$. Then, Algorithm 2 outputs $\tilde{\theta}_K$ satisfies

$$\mathbb{E} \left[\left\| \mathcal{G}_{\alpha, \langle -\nabla J(\tilde{\theta}_K), \theta \rangle}^{\psi}(\tilde{\theta}_K) \right\| \right] \leq \epsilon. \quad (30)$$

For its proof, see Appendix D.

Theorem 4.1 illustrates that VRMPO needs

$$\begin{aligned} & K(N_1 + (m - 1)N_2) \\ &= \frac{8L(\mathbb{E}[\mathcal{J}(\tilde{\theta}_0)] - \mathcal{J}(\theta^*))}{\left(\zeta - \frac{5}{32}\right)} \left(1 + \frac{1}{16\zeta^2}\right) \left(1 + \sqrt{\left(\frac{1}{8L\zeta^2} + \frac{1}{2(\zeta - \frac{5}{32})} \left(1 + \frac{1}{32\zeta^2}\right)\right) \frac{\sigma}{\epsilon}}\right) \frac{1}{\epsilon^2} = \mathcal{O}\left(\frac{1}{\epsilon^3}\right) \end{aligned}$$

random trajectories to achieve the ϵ -FOSP. As far as we know, our VRMPO matches the best sample complexity as HAPG [Shen et al., 2019] and SRVR-PG [Xu et al., 2020; Xu, 2021]. In fact, according to Shen et al. [2019], REINFORCE needs $\mathcal{O}(\epsilon^{-4})$ random trajectories to achieve the ϵ -FOSP, and no provable improvement on its complexity has been made so far. The same order of sample complexity

Algorithm	Conditions	Complexity
VPG and REINFORCE	Assumption 2.1, $\text{Var}[g(\tau \theta)] < +\infty$	$\mathcal{O}(\epsilon^{-4})$
TRPO [Shani et al., 2020]	Assumption 2.1	$\mathcal{O}(\epsilon^{-4})$
TRPO [Liu et al., 2019]	Assumption 2.1	$\mathcal{O}(\epsilon^{-8})$
SVRPG Papini et al. [2018]	Assumption 2.1, $\text{Var}[\rho_t] < +\infty, \text{Var}[g(\tau \theta)] < +\infty$	$\mathcal{O}(\epsilon^{-4})$
SVRPG Xu et al. [2019]	Assumption 2.1; $\text{Var}[\rho_t] < +\infty, \text{Var}[g(\tau \theta)] < +\infty$	$\mathcal{O}(\epsilon^{-10/3})$
HAPG [Shen et al., 2019]	Assumption 2.1	$\mathcal{O}(\epsilon^{-3})$
SRVR-PG [Xu et al., 2020; Xu, 2021]	Assumption 2.1; $\text{Var}[\rho_t] < +\infty; \text{Var}[g(\tau \theta)] < +\infty$	$\mathcal{O}(\epsilon^{-3})$
VR-PGPO [Huang et al., 2021]	Assumption 2.1; $\text{Var}[\rho_t] < +\infty; \text{Var}[g(\tau \theta)] < +\infty$	$\mathcal{O}(\epsilon^{-3})$
VRMPO (Our Work)	Assumption 2.1	$\mathcal{O}(\epsilon^{-3})$

Table 1: Comparison of complexity achieves $\|\nabla J(\theta)\| \leq \epsilon$. If $\psi(\theta) = \frac{1}{2}\|\theta\|_2^2$, then the result (41) of our VRMPO is also measured by gradient. Beside, $\rho_t \stackrel{\text{def}}{=} \prod_{i=0}^H \frac{\pi_{\theta_0}(a_i|s_i)}{\pi_{\theta_t}(a_i|s_i)}$.

of REINFORCE is shown by Xu et al. [2019]. With the additional assumptions

$$\text{Var} \left[\prod_{h=0}^H \frac{\pi_{\theta_0}(a_h|s_h)}{\pi_{\theta_t}(a_h|s_h)} \right], \quad \text{Var}[g(\tau|\theta)] < +\infty,$$

Papini et al. [2018] show that the SVRPG achieves the sample complexity of $\mathcal{O}(\epsilon^{-4})$. Later, under the same assumption as Papini et al. [2018], Xu et al. [2019] reduce the sample complexity of SVRPG to $\mathcal{O}(\epsilon^{-\frac{10}{3}})$. We summarize it in Table 1.

Remark 4.1. *It’s remarkable that although our VRMPO shares sample complexity with HAPG, SRVR-PG, and VR-BGPO [Huang et al., 2021], the difference between our VRMPO and theirs are at least three aspects:*

- ❶ *Shen et al. [2019] derive their HAPG from the information of Hessian policy, our VRMPO provides a simple recursive formulation to conduct the gradient estimator.*
- ❷ *If the mirror map ψ is reduced to the ℓ_2 -norm, then VRMPO is SRVR-PG exactly, i.e., VRMPO unifies SRVR-PG. From Table 1, we see VRMPO needs less conditions than Xu et al. [2020] to achieve the same sample complexity.*
- ❸ *Shen et al. [2019], Xu et al. [2020] and Huang et al. [2021] only provide an off-line (i.e., Monte Carlo) policy gradient estimator, which is limited in complex domains. We have provided an on-line version of VRMPO, and discuss some insights of practical tracks to the application to the complex domains, please see the section of experiment on MuJoCo task, Appendix E.1 and Algorithm 3.*

5 Related Works

5.1 Stochastic Variance Reduced Gradient in RL

To our best knowledge, Du et al. [2017] firstly introduce SVRG Johnson and Zhang [2013] to off-policy evaluation. Du et al. [2017] transform the empirical policy evaluation problem into a convex-concave saddle-point problem, then they solve the problem via SVRG straightforwardly. Later, to improve sample efficiency for complex RL, Xu et al. [2017] combine SVRG with TRPO [Schulman et al., 2015]. Similarly, Yuan et al. [2019] introduce SARAH [Nguyen et al., 017a] to TRPO to improve sample efficiency. However, the results presented by Xu et al. [2017] and Yuan et al. [2019] are empirical,

which lacks a strong theory analysis. Metelli et al. [2018] present a surrogate objective function with Rényi divergence [Rényi et al., 1961] to reduce the variance. Recently, Papini et al. [2018] propose a stochastic variance reduced version of policy gradient (SVRPG), and they define the gradient estimator via importance sampling as: for each step k ,

$$\tilde{G}_{k-1} + \frac{1}{N} \sum_{j=1}^N \left(-g(\tau_j^k | \theta_t) + \prod_{i=0}^H \frac{\pi_{\theta_0}(a_i | s_i)}{\pi_{\theta_t}(a_i | s_i)} g(\tau_j^k | \theta_{t-1}) \right),$$

where \tilde{G}_{k-1} is an unbiased estimator according to the trajectory generated by $\pi_{\theta_{k-1}}$. Although SVRPG is practical empirically, its gradient estimate is dependent heavily on importance sampling. This fact partially reduces the effectiveness of variance reduction. Later, Shen et al. [2019] remove the importance sampling term, and they construct a Hessian aided policy gradient.

Our VRMPO is different from Du et al. [2017]; Xu et al. [2017]; Papini et al. [2018], which admits a stochastic recursive iteration to estimate the policy gradient. VRMPO exploits fresh information to improve convergence and reduces variance. Besides, VRMPO reduces the storage cost since it doesn't require to store the complete historical information.

5.2 Baseline Methods

Baseline (also also known as control variates) is a widely used technique to reduce the variance [Weaver and Tao, 2001; Greensmith et al., 2004]. For example, A2C [Sutton and Barto, 1998; Mnih et al., 2016] introduces the value function as baseline function, Wu et al. [2018] consider action-dependent baseline, and Liu et al. [2018] use the Stein's identity [Stein, 1986] as baseline. Q-Prop [Gu et al., 2017] makes use of both the linear dependent baseline and GAE Schulman et al. [2016] to reduce variance. Cheng et al. [2019b] present a predictor-corrector framework transforms a first-order model-free algorithm into a new hybrid method that leverages predictive models to accelerate policy learning. Mao et al. [2019] derive a bias-free, input-dependent baseline to reduce variance, and analytically show its benefits over state-dependent baselines. Recently, Grathwohl et al. [2018]; Cheng et al. [2019a] provide a standard explanation for the benefits of such approaches with baseline function.

However, the capacity of all the above methods is limited by their choice of baseline function [Liu et al., 2018]. In practice, it is troublesome to design a proper baseline function to reduce the variance of policy gradient estimate. Our VRMPO avoids the selection of baseline function, and it uses the current trajectories to construct a novel, efficiently computable gradient to reduce variance and improve sample efficiency.

6 Experiments

Our experiments cover the following three different aspects:

- We provide a numerical analysis of MPO, and compare the convergence rate of MPO with REINFORCE and VPG on the *Short Corridor with Switched Actions* (SASC) domain [Sutton and Barto, 2018].
- We provide a better understand the effect of how the mirror map affects the performance of VRMPO.
- To demonstrate the stability and efficiency of VRMPO on the MuJoCo continuous control tasks, we provide a comprehensive comparison to state-of-the-art policy optimization algorithms.

6.1 Numerical Analysis of MPO

SASC Domain (see Appendix B): The task is to estimate the optimal value function of state \mathbf{s}_1 , $V(\mathbf{s}_1) = G_0 \approx -11.6$. Let $\phi(s, \mathbf{right}) = [1, 0]^\top$ and $\phi(s, \mathbf{left}) = [0, 1]^\top$, $s \in \mathcal{S}$. Let $L_\theta(s, a) = \phi^\top(s, a)\theta$, $(s, a) \in \mathcal{S} \times \mathcal{A}$, where $\mathcal{A} = \{\mathbf{right}, \mathbf{left}\}$. $\pi_\theta(a|s)$ is the soft-max distribution defined as

$$\pi_\theta(a|s) = \frac{\exp\{L_\theta(s, a)\}}{\sum_{a' \in \mathcal{A}} \exp\{L_\theta(s, a')\}}.$$

The initial parameter $\theta_0 \sim \mathcal{U}[-0.5, 0.5]$, where \mathcal{U} is the uniform distribution.

Before we report the results, it is necessary to explain why we only compare MPO with VPG and REINFORCE. VPG/REINFORCE is one of the most fundamental policy gradient methods in RL, and extensive modern policy-based algorithms are derived from VPG/REINFORCE. Our MPO is a new policy gradient algorithm to learn the parameter. Thus, it is natural to compare with VPG and REINFORCE. The result of Figure 1 shows that MPO converges faster significantly than both REINFORCE and VPG.

6.2 Effect of Mirror Map on VRMPO

If $\psi(\cdot)$ is ℓ_p -norm, then $\psi^*(y) = (\sum_{i=1}^n |y_i|^q)^{\frac{1}{q}}$ is the conjugate map of ψ , where $y = (y_1, y_2, \dots, y_n)^\top$, $\frac{1}{p} + \frac{1}{q} = 1$, and $p, q > 1$. According to Beck and Teboulle [2003], iteration (27) is equivalent to

$$\theta_{k+1} = \nabla \psi^*(\nabla \psi(\theta_k) + \alpha G_k),$$

where $\nabla \psi_j(x)$ and $\nabla \psi_j^*(y)$ are:

$$\nabla \psi_j(x) = \frac{\text{sign}(x_j)|x_j|^{p-1}}{\|x\|_p^{p-2}}, \nabla \psi_j^*(y) = \frac{\text{sign}(y_j)|y_j|^{q-1}}{\|y\|_q^{q-2}},$$

and j is coordinate index of the vector $\nabla \psi$, $\nabla \psi^*$.

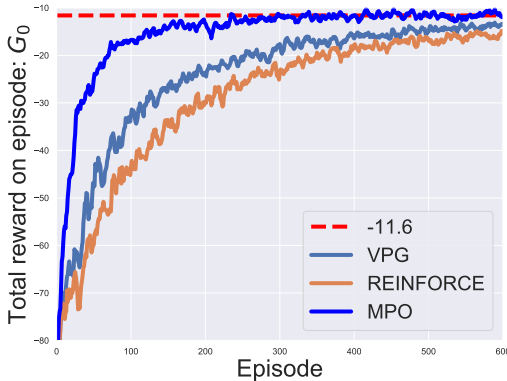


Figure 1: Convergence comparison between our MPO algorithm and REINFORCE/VPG on the SASC domain.

To compare fairly, we use the same random seed for each domain. The hyper-parameter p runs in the set $[P] = \{1.1, 1.2, \dots, 1.9, 2, 3, 4, 5\}$. For the non-Euclidean distance case, we only show the results of $p = 3, 4, 5$ in Figure 2, and “best” is a certain hyper-parameter $p \in [P]$ achieves the best performance among the set $[P]$. We use a two-layer feedforward neural network of 200 and

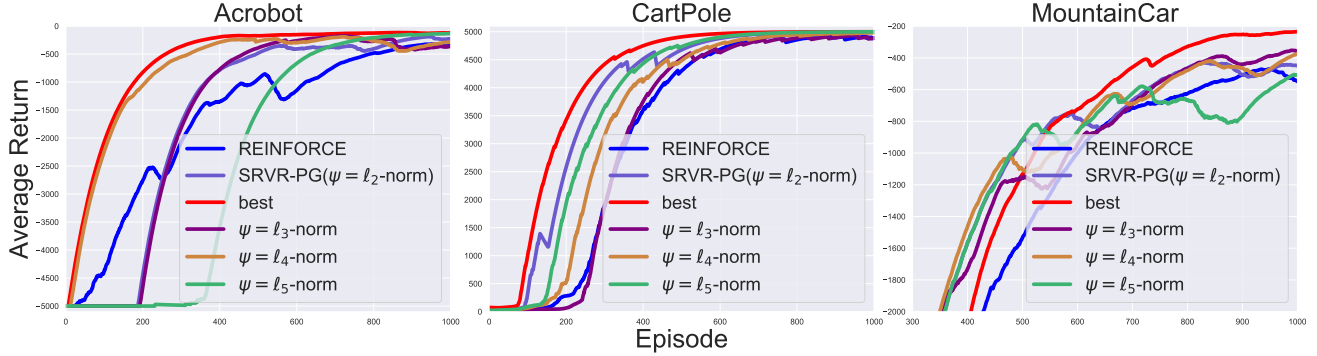


Figure 2: Comparison of the empirical performance of VRMPO between different mirror maps and REINFORCE.

100 hidden nodes, respectively, with rectified linear units (ReLU) activation function between each layer. We run the discount $\gamma = 0.99$ and the step-size α is chosen by a grid search from the set $\{0.01, 0.02, 0.04, 0.08, 0.1\}$.

The result of Figure 2 shows that the best method is produced by non-Euclidean distance ($p \neq 2$), not the Euclidean distance ($p = 2$). The traditional policy gradient methods such as REINFORCE, VPG, and DPG are all the algorithms update parameters by Euclidean distance. This experiment gives us some light that one can create better algorithms with existing approaches via non-Euclidean distance. Additionally, the result of Figure 2 shows our VRMPO converges faster than REINFORCE, i.e., VRMPO needs less sampled trajectories to reach a convergent state, which supports the complexity analysis in Table 1. Although SRVR-PG achieves the same sample complexity as our VRMPO, result of Figure 2 shows VRMPO converges faster than SRVR-PG.

6.3 Evaluate VRMPO on Continuous Control Tasks

It is noteworthy that the policy gradient (26) of VRMPO is an off-line estimator likes REINFORCE. As pointed by Sutton and Barto [2018], REINFORCE converge asymptotically to a local minimum, but like all off-line methods, it is inconvenient for continuous control tasks, and it is limited in the application to some complex domains. This could also happen in VRMPO.

Now, we introduce some practical tricks for on-line implementation of VRMPO. We have provided the complete update rule of on-line VRMPO in Algorithm 3.

Details of Implementation. Firstly, we extend Algorithm 2 to be an actor-critic structure, i.e., we introduce a critic structure to Algorithm 2. Concretely, for each step t , we construct a critic network $Q_\omega(s, a)$ with the parameter ω , sample $\{(s_i, a_i)\}_{i=1}^N$ from a data memory \mathcal{D} , and learn the parameter ω via minimizing the critic loss as follows,

$$L_\omega = \frac{1}{N} \sum_{i=1}^N (r_{i+1} + \gamma Q_{\omega_{k-1}}(s_i, a_i) - Q_\omega(s_i, a_i))^2. \quad (31)$$

For more details, please see Line 17-20 of Algorithm 3. Then, for each pair $(s, a) \sim \mathcal{D}$, we conduct the actor loss

$$L_\theta(s, a) = -\log \pi_\theta(s, a) Q_{\omega_{k-1}}(s, a)$$

to replace $J(\theta)$ to learn parameter θ . For more details, please see Line 9-16 of Algorithm 3 (Appendix E.1).

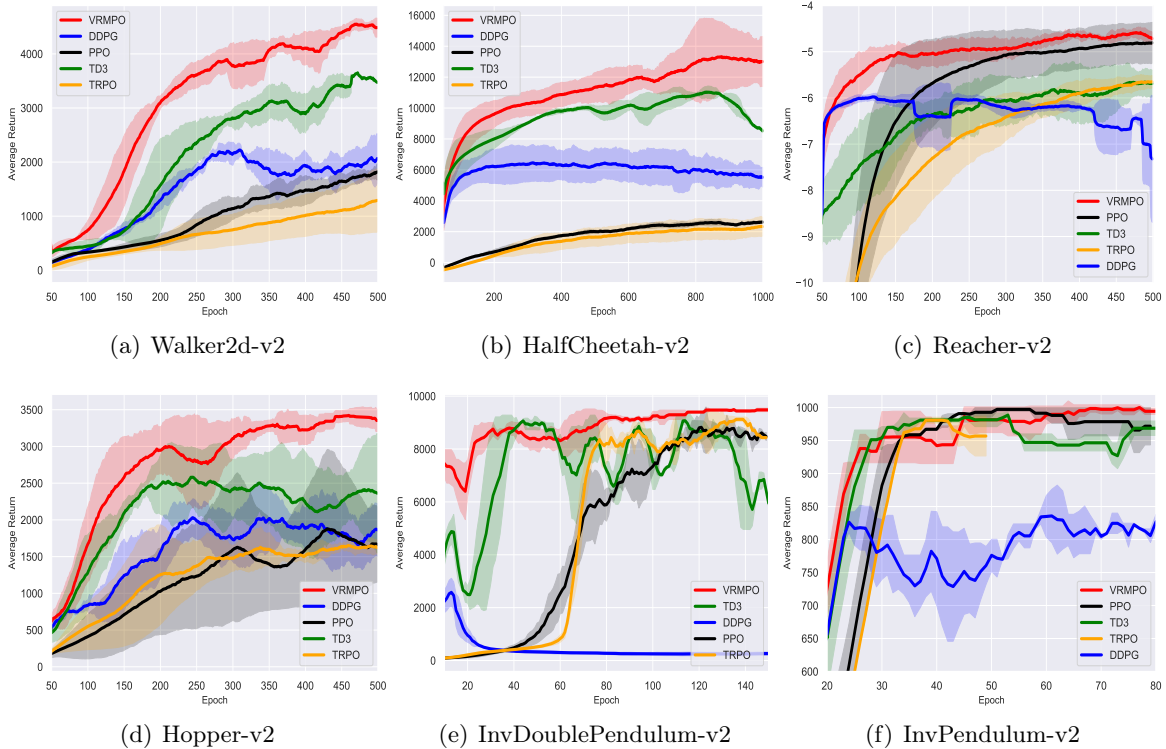


Figure 3: Learning curves for continuous control tasks. The shaded region represents the standard deviation of the score over the best three trials. Curves are smoothed uniformly for visual clarity.

Environment	VRMPO	TD3	DDPG	PPO	TRPO
Walker2d	5251.83	4887.85	5795.13	3905.99	3636.59
HalfCheetah	16095.51	11781.07	8616.29	3542.60	3325.23
Reacher	-0.49	-1.47	-1.55	-0.44	-0.66
Hopper	3751.43	3482.06	3558.69	3609.65	3578.06
InvPendulum	9359.82	9248.27	6958.42	9045.86	9151.56
InvPendulum	1000.00	1000.00	907.81	1000.00	1000.00

Table 2: Max-average return over final 50 epochs, where we run 5000 iterations for each epoch. Maximum value for each task is bolded.

Score Performance Comparison.

From the results of Figure 3 and Table 2, overall, VRMPO outperforms the baseline algorithms in both final performance and learning process. Our VRMPO also learns considerably faster with better performance than the popular TD3 on Walker2d, HalfCheetah, Hopper, InvDoublePendulum (IDP), and Reacher domains. On the InvDoublePendulum task, our VRMPO has only a small advantage over other algorithms. This is because the InvPendulum task is relatively easy. The advantage of our VRMPO becomes more powerful when the task is more difficult. It is worth noticing that on the HalfCheetah domain, our VRMPO achieves a significant max-average score 16000+, which outperforms far more than the second-best score 11781.

Stability.

The stability of an algorithm is also an important topic in RL. Although DDPG exploits the off-policy

samples, which promotes its efficiency in stable environments. DDPG is unstable on the Reacher task, while our VRMPO learning faster significantly with lower variance. DDPG fails to make any progress on InvDoublePendulum domain, which is corroborated by Dai et al. [2018]. Although TD3 takes the minimum value between a pair of critics to limit overestimation, it learns severely fluctuating in the InvertedDoublePendulum environment. In contrast, our VRMPO is consistently reliable and effective in different tasks.

Variance Comparison.

As we can see from the results in Figure 3, our VRMPO converges with a considerably low variance in the Hopper, InvDoublePendulum, and Reacher. Although the asymptotic variance of VRMPO is slightly larger than other algorithms in HalfCheetah, the final performance of VRMPO outperforms all the baselines significantly. The result of Figure 3 also implies conducting a proper gradient estimator not only reduces the variance of the score during the learning but speeds the convergence of training.

7 Conclusion

In this paper, we analyze the theoretical dilemma of applying SMD to policy optimization. Then, we propose a sample efficient algorithm VRMPO, and prove the sample complexity of VRMPO achieves only $\mathcal{O}(\epsilon^{-3})$. To our best knowledge, VRMPO matches the best sample complexity so far. Finally, we conduct extensive experiments to show our algorithm outperforms state-of-the-art policy gradient methods.

References

- Agarwal, A., Kakade, S. M., Lee, J. D., and Mahajan, G. (2020). Optimality and approximation with policy gradient methods in markov decision processes. *COLT*.
- Bauschke, H. H., Combettes, P. L., et al. (2011). *Convex analysis and monotone operator theory in Hilbert spaces*, volume 408.
- Beck, A. and Teboulle, M. (2003). Mirror descent and nonlinear projected subgradient methods for convex optimization. *Operations Research Letters*, 31(3):167–175.
- Bertsekas, D. P. (2009). *Convex optimization theory*. Athena Scientific Belmont.
- Cheng, C.-A., Yan, X., and Boots, B. (2019a). Trajectory-wise control variates for variance reduction in policy gradient methods. *ICRA*.
- Cheng, C.-A., Yan, X., Ratliff, N., and Boots, B. (2019b). Predictor-corrector policy optimization. In *ICML*.
- Dai, B., Shaw, A., Li, L., Xiao, L., He, N., Liu, Z., Chen, J., and Song, L. (2018). Sbeed: Convergent reinforcement learning with nonlinear function approximation. *ICML*.
- Du, S. S., Chen, J., Li, L., Xiao, L., and Zhou, D. (2017). Stochastic variance reduction methods for policy evaluation. In *ICML*.
- Duan, Y., Chen, X., Houthoofd, R., Schulman, J., and Abbeel, P. (2016). Benchmarking deep reinforcement learning for continuous control. In *ICML*.
- Fujimoto, S., van Hoof, H., Meger, D., et al. (2018). Addressing function approximation error in actor-critic methods. *ICML*.
- Ghadimi, S., Lan, G., and Zhang, H. (2016). Mini-batch stochastic approximation methods for nonconvex stochastic composite optimization. *Mathematical Programming*, 155(1-2):267–305.
- Grathwohl, W., Choi, D., Wu, Y., Roeder, G., and Duvenaud, D. (2018). Backpropagation through the void: Optimizing control variates for black-box gradient estimation. *ICLR*.
- Greensmith, E., Bartlett, P. L., Baxter, J., et al. (2004). Variance reduction techniques for gradient estimates in reinforcement learning. *JMLR*, 5(Nov):1471–1530.
- Gu, S., Lillicrap, T., Ghahramani, Z., Turner, R. E., and Levine, S. (2017). Q-prop: Sample-efficient policy gradient with an off-policy critic. *ICLR*.
- Haarnoja, T., Zhou, A., Abbeel, P., and Levine, S. (2018). Soft actor-critic: Off-policy maximum entropy deep reinforcement learning with a stochastic actor. In *ICML*.
- Huang, F., Gao, S., Huang, H., and et.al (2021). Bregman gradient policy optimization. *arXiv preprint arXiv:2106.12112*.
- Jain, P., Kar, P., et al. (2017). Non-convex optimization for machine learning. *Foundations and Trends® in Machine Learning*, 10(3-4):142–336.
- Johnson, R. and Zhang, T. (2013). Accelerating stochastic gradient descent using predictive variance reduction. In *NeurIPS*, pages 315–323.
- Kakade, S. M. (2002). A natural policy gradient. In *NeurIPS*, pages 1531–1538.
- Kingma, D. P. and Ba, J. (2015). Adam: A method for stochastic optimization. *ICLR*.

- Konda, V. R. and Tsitsiklis, J. N. (2000). Actor-critic algorithms. In *NeurIPS*, pages 1008–1014.
- Lei, Y. and Tang, K. (2018). Stochastic composite mirror descent: optimal bounds with high probabilities. In *NeurIPS*, pages 1519–1529.
- Liu, B., Cai, Q., Yang, Z., and Wang, Z. (2019). Neural proximal/trust region policy optimization attains globally optimal policy. *NeurIPS*.
- Liu, H., Feng, Y., Mao, Y., Zhou, D., Peng, J., and Liu, Q. (2018). Action-dependent control variates for policy optimization via stein identity. *ICLR*.
- Mao, H., Venkatakrisnan, S. B., Schwarzkopf, M., and Alizadeh, M. (2019). Variance reduction for reinforcement learning in input-driven environments. *ICLR*.
- Meng, W., Zheng, Q., Yang, L., Li, P., and Pan, G. (2019). Qualitative measurements of policy discrepancy for return-based deep q-network. *IEEE transactions on neural networks and learning systems*, 31(10):4374–4380.
- Metelli, A. M., Papini, M., Faccio, F., and Restelli, M. (2018). Policy optimization via importance sampling. In *NeurIPS*, pages 5442–5454.
- Mnih, V., Badia, A. P., Mirza, M., Graves, A., Lillicrap, T., Harley, T., Silver, D., and Kavukcuoglu, K. (2016). Asynchronous methods for deep reinforcement learning. In *ICML*, pages 1928–1937.
- Nemirovsky, A. S. and Yudin, D. B. (1983). Problem complexity and method efficiency in optimization.
- Nguyen, L. M., Liu, J., Scheinberg, K., and Takáč, M. (2017a). Sarah: A novel method for machine learning problems using stochastic recursive gradient. In *ICML*.
- Papini, M., Binaghi, D., Canonaco, G., and Matteo Pirodda, M. R. (2018). Stochastic variance-reduced policy gradient. In *ICML*.
- Peters, J., Mülling, K., Altun, and Yasemin (2010). Relative entropy policy search. In *AAAI*, pages 1607–1612.
- Reddi, S. J., Hefny, A., Sra, S., Póczos, B., and Smola, A. (2016). Stochastic variance reduction for nonconvex optimization. In *ICML*, pages 314–323.
- Rényi, A. et al. (1961). On measures of entropy and information. In *Proceedings of the Fourth Berkeley Symposium on Mathematical Statistics and Probability, Volume 1: Contributions to the Theory of Statistics*.
- Schulman, J., Levine, S., Abbeel, P., Jordan, M., and Moritz, P. (2015). Trust region policy optimization. In *ICML*, pages 1889–1897.
- Schulman, J., Moritz, P., Levine, S., Jordan, M., and Abbeel, P. (2016). High-dimensional continuous control using generalized advantage estimation. *ICLR*.
- Shani, L., Efroni, Y., Mannor, S., and et.al (2020). Adaptive trust region policy optimization: Global convergence and faster rates for regularized mdps. In *AAAI*, volume 34, pages 5668–5675.
- Shen, Z., Ribeiro, A., Hassani, H., Qian, H., and Mi, C. (2019). Hessian aided policy gradient. In *ICML*, pages 5729–5738.
- Silver, D., Huang, A., Maddison, C. J., Guez, A., Sifre, L., Van Den Driessche, G., Schrittwieser, J., Antonoglou, I., Panneershelvam, V., Lanctot, M., et al. (2016). Mastering the game of go with deep neural networks and tree search. *nature*, 529(7587):484–489.

- Silver, D., Lever, G., Heess, N., Degris, T., Wierstra, D., and Riedmiller, M. (2014). Deterministic policy gradient algorithms. In *ICML*.
- Silver, D., Schrittwieser, J., Simonyan, K., Antonoglou, I., Huang, A., Guez, A., Hubert, T., Baker, L., Lai, M., Bolton, A., et al. (2017). Mastering the game of go without human knowledge. *Nature*, 550(7676):354.
- Stein, C. (1986). Approximate computation of expectations. *Lecture Notes-Monograph Series*, 7:i–164.
- Sutton, R. S. and Barto, A. G. (1998). *Reinforcement learning: An introduction*. MIT press.
- Sutton, R. S. and Barto, A. G. (2018). *Reinforcement learning: An introduction*. MIT press.
- Sutton, R. S., McAllester, D. A., Singh, S. P., and Mansour, Y. (2000). Policy gradient methods for reinforcement learning with function approximation. In *NeurIPS*, pages 1057–1063.
- Tomar, M., Shani, L., Efroni, Y., and Ghavamzadeh, M. (2020). Mirror descent policy optimization. *arXiv preprint arXiv:2005.09814*.
- Van Hasselt, H., Guez, A., and Silver, D. (2016). Deep reinforcement learning with double q-learning. In *AAAI*.
- Weaver, L. and Tao, N. (2001). The optimal reward baseline for gradient-based reinforcement learning. In *UAI*, pages 538–545. Morgan Kaufmann Publishers Inc.
- Williams, R. J. (1992). Simple statistical gradient-following algorithms for connectionist reinforcement learning. *Machine learning*, 8(3-4):229–256.
- Wu, C., Rajeswaran, A., Duan, Y., Kumar, V., Bayen, A. M., Kakade, S., Mordatch, I., and Abbeel, P. (2018). Variance reduction for policy gradient with action-dependent factorized baselines. *ICLR*.
- Xing, D., Liu, Q., Zheng, Q., and Pan, G. (2021). Learning with generated teammates to achieve type-free ad-hoc teamwork. In *IJCAI*.
- Xu, P. (2021). *Sample-Efficient Nonconvex Optimization Algorithms in Machine Learning and Reinforcement Learning*. PhD thesis, UCLA.
- Xu, P., Gao, F., Gu, Q., et al. (2019). An improved convergence analysis of stochastic variance-reduced policy gradient. *UAI*.
- Xu, P., Gao, F., Gu, Q., et al. (2020). Sample efficient policy gradient methods with recursive variance reduction. *ICLR*.
- Xu, T., Liu, Q., and Peng, J. (2017). Stochastic variance reduction for policy gradient estimation. *arXiv preprint arXiv:1710.06034*.
- Yang, L., Zheng, Q., and Pan, G. (2021). Sample complexity of policy gradient finding second-order stationary points. *AAAI2021*.
- Yuan, H., Li, C. J., Tang, Y., and Zhou, Y. (2019). Policy optimization via stochastic recursive gradient algorithm. <https://openreview.net/forum?id=rJl3S2A9t7>.

A Notations

For convenience of reference, we list some key notations that have been used in this paper.

- $J(\theta)$: The expected return function.
- $\mathcal{J}(\theta)$: $\mathcal{J}(\theta) = -J(\theta)$.
- L : The Lipschitz constant, see (5).
- σ : The boundedness of the variance of the policy gradient estimator, see (6).
- ψ : The mirror map.
- ζ : The mirror map ψ is a ζ -strictly convex function, and we present it in Definition 2.1.
- $\mathcal{G}(\cdot)$: Bregman gradient, see (10).
- Δ : $\Delta = J(\theta^*) - J(\theta_1)$.

B Appendix A: Proof of Theorem 3.2

Theorem 3.2 (Convergence Rate of Algorithm 1) *Under Assumption 2.1, and the total trajectories are $\{\tau_k\}_{k=1}^N$. Consider the sequence $\{\theta_k\}_{k=1}^N$ generated by Algorithm 1, and the output $\theta_N = \theta_n$ follows the distribution of Eq.(16). Let $0 < \alpha_k < \frac{\zeta}{L}$, $\ell(g, u) = \langle g, u \rangle$. Let $\hat{g}_k = \frac{1}{k} \sum_{i=1}^k g_i$, where $g_i = \sum_{t=0}^{H_{\tau_i}} \nabla_{\theta} \log \pi_{\theta}(a_t | s_t) R(\tau_i) |_{\theta=\theta_i}$. Then we have*

$$\mathbb{E}[\|\mathcal{G}_{\alpha_n, \ell(-g_n, \theta_n)}^{\psi}(\theta_n)\|^2] \leq \frac{(J(\theta^*) - J(\theta_1)) + \frac{\sigma^2}{\zeta} \sum_{k=1}^N \frac{\alpha_k}{k}}{\sum_{k=1}^N (\zeta \alpha_k - L \alpha_k^2)}.$$

Let $f(\theta)$ be a L -smooth function defined on \mathbb{R}^n , i.e. $\|\nabla f(\theta) - \nabla f(\theta')\| \leq L\|\theta - \theta'\|$. Then, according to Jain et al. [2017], for $\forall \theta, \theta' \in \mathbb{R}^n$, the following holds

$$\|f(\theta) - f(\theta') - \langle \nabla f(\theta'), \theta - \theta' \rangle\| \leq \frac{L}{2} \|\theta - \theta'\|^2. \quad (32)$$

Lemma B.1 (Ghadimi et al. [2016], Lemma 1 and Proposition 1). *Let \mathcal{X} be a closed convex set in \mathbb{R}^d , $f(\theta)$ is a L -smooth function defined on \mathcal{X} , $h(\cdot) : \mathcal{X} \rightarrow \mathbb{R}$ be a convex function, but possibly nonsmooth, and $D_{\psi} : \mathcal{X} \times \mathcal{X} \rightarrow \mathbb{R}$ is Bregman divergence. Moreover, we define*

$$\begin{aligned} \theta^+ &= \arg \min_{u \in \mathcal{X}} \{ \langle g, u \rangle + \frac{1}{\alpha} D_{\psi}(u, \theta) + h(u) \} \\ P_{\mathcal{X}}(\theta, g, \alpha) &= \frac{1}{\alpha} (\theta - \theta^+), \end{aligned} \quad (33)$$

where $g = \nabla f(\theta) \in \mathbb{R}^d$, $\theta \in \mathcal{X}$, and $\alpha > 0$. Then, the following statement holds

$$\langle g, P_{\mathcal{X}}(\theta, g, \alpha) \rangle \geq \zeta \|P_{\mathcal{X}}(\theta, g, \alpha)\|^2 + \frac{1}{\alpha} [h(\theta^+) - h(\theta)], \quad (34)$$

where ζ is a positive constant determined by ψ (i.e. ψ is a continuously-differentiable and ζ -strictly convex function) that satisfies $\langle \theta - \theta', \nabla \psi(\theta) - \nabla \psi(\theta') \rangle \geq \zeta \|\theta - \theta'\|^2$. Moreover, for any $g_1, g_2 \in \mathbb{R}^d$, the following statement holds

$$\|P_{\mathcal{X}}(\theta, g_1, \alpha) - P_{\mathcal{X}}(\theta, g_2, \alpha)\| \leq \frac{1}{\zeta} \|g_1 - g_2\|. \quad (35)$$

Remark B.1. Ghadimi, Lan, and Zhang Ghadimi et al. [2016] call $P_{\mathcal{X}}(\theta, g, \alpha)$ (33) projected gradient. It is noteworthy that if $h(\cdot) = 0$, then the projected gradient $P_{\mathcal{X}}(x, g, \alpha)$ is reduced to Bregman Gradient (10). Concretely, for Eq.(33), let $h(\cdot) \equiv 0$, then we have

$$P_{\mathcal{X}}(\theta, g, \alpha) \stackrel{(33)}{=} \frac{1}{\alpha} \left(\theta - \arg \min_{u \in \mathcal{X}} \{ \langle g, u \rangle + \frac{1}{\alpha} D_{\psi}(u, \theta) \} \right) \stackrel{(10)}{=} \mathcal{G}_{\alpha, \langle g, \theta \rangle}^{\psi}(\theta).$$

Proof. (Proof of Theorem 3.2)

Let $\mathcal{T} = \{\tau_k\}_{k=1}^N$, at each terminal end of a trajectory $\tau_k = \{s_t, a_t, r_{t+1}\}_{t=0}^{H_{\tau_k}} \in \mathcal{T}$, let $g_k = \sum_{t=0}^{H_{\tau_k}} \nabla_{\theta} \log \pi_{\theta}(a_t | s_t) R(\tau_k) |_{\theta=\theta_k}$, $\hat{g}_k = \frac{1}{k} \sum_{i=1}^k g_i$, according to Algorithm 1, at the terminal end of k -th episode, $k = 1, 2, \dots, N$, the following holds,

$$\theta_{k+1} = \arg \min_{\theta} \{ \langle -\hat{g}_k, \theta \rangle + \frac{1}{\alpha_k} D_{\psi}(\theta, \theta_k) \} = \mathcal{M}_{\alpha_k, \ell(-\hat{g}_k, \theta)}^{\psi}(\theta_k).$$

To simplify expression, let $\mathcal{J}(\theta) = -J(\theta)$. Then $\mathcal{J}(\theta)$ is also a L -smooth function, according to Eq.(32), we have

$$\begin{aligned} \mathcal{J}(\theta_{k+1}) &\leq \mathcal{J}(\theta_k) + \langle \nabla \mathcal{J}(\theta) |_{\theta=\theta_k}, \theta_{k+1} - \theta_k \rangle + \frac{L}{2} \|\theta_{k+1} - \theta_k\|^2 \\ &= \mathcal{J}(\theta_k) - \alpha_k \langle \nabla \mathcal{J}(\theta_k), \mathcal{G}_{\alpha_k, \ell(-\hat{g}_k, \theta_k)}^{\psi}(\theta_k) \rangle + \frac{L\alpha_k^2}{2} \|\mathcal{G}_{\alpha_k, \ell(-\hat{g}_k, \theta_k)}^{\psi}(\theta_k)\|^2 \\ &= \mathcal{J}(\theta_k) - \alpha_k \langle \hat{g}_k, \mathcal{G}_{\alpha_k, \ell(-\hat{g}_k, \theta_k)}^{\psi}(\theta_k) \rangle + \frac{L\alpha_k^2}{2} \|\mathcal{G}_{\alpha_k, \ell(-\hat{g}_k, \theta_k)}^{\psi}(\theta_k)\|^2 + \alpha_k \langle \epsilon_k, \mathcal{G}_{\alpha_k, \ell(-\hat{g}_k, \theta_k)}^{\psi}(\theta_k) \rangle, \end{aligned}$$

where $\epsilon_k = -\hat{g}_k - (-\nabla J(\theta_k)) = -\hat{g}_k - \nabla \mathcal{J}(\theta_k)$.

Furthermore, by Eq.(34), let $\alpha = \alpha_k$ and $g = -\hat{g}_k$, then we have

$$\begin{aligned} \mathcal{J}(\theta_{k+1}) &\leq \mathcal{J}(\theta_k) - \alpha_k \zeta \|\mathcal{G}_{\alpha_k, \ell(-\hat{g}_k, \theta_k)}^{\psi}(\theta_k)\|^2 + \frac{L\alpha_k^2}{2} \|\mathcal{G}_{\alpha_k, \ell(-\hat{g}_k, \theta_k)}^{\psi}(\theta_k)\|^2 + \alpha_k \langle \epsilon_k, \mathcal{G}_{\alpha_k, \ell(-\hat{g}_k, \theta_k)}^{\psi}(\theta_k) \rangle \\ &= \mathcal{J}(\theta_k) - \alpha_k \zeta \|\mathcal{G}_{\alpha_k, \ell(-\hat{g}_k, \theta_k)}^{\psi}(\theta_k)\|^2 + \frac{L\alpha_k^2}{2} \|\mathcal{G}_{\alpha_k, \ell(-\hat{g}_k, \theta_k)}^{\psi}(\theta_k)\|^2 + \alpha_k \langle \epsilon_k, \mathcal{G}_{\alpha_k, \ell(-\nabla J(\theta_k), \theta_k)}^{\psi}(\theta_k) \rangle \\ &\quad + \alpha_k \langle \epsilon_k, \mathcal{G}_{\alpha_k, \ell(-\hat{g}_k, \theta_k)}^{\psi}(\theta_k) - \mathcal{G}_{\alpha_k, \ell(-\nabla J(\theta_k), \theta_k)}^{\psi}(\theta_k) \rangle. \end{aligned} \tag{36}$$

Rearranging Eq.(36), we have

$$\begin{aligned} \mathcal{J}(\theta_{k+1}) &\leq \mathcal{J}(\theta_k) - \left(\zeta \alpha_k - \frac{L\alpha_k^2}{2} \right) \|\mathcal{G}_{\alpha_k, \ell(-\hat{g}_k, \theta_k)}^{\psi}(\theta_k)\|^2 + \alpha_k \langle \epsilon_k, \mathcal{G}_{\alpha_k, \ell(-\nabla J(\theta_k), \theta_k)}^{\psi}(\theta_k) \rangle \\ &\quad + \alpha_k \|\epsilon_k\| \|\mathcal{G}_{\alpha_k, \ell(-\hat{g}_k, \theta_k)}^{\psi}(\theta_k) - \mathcal{G}_{\alpha_k, \ell(-\nabla J(\theta_k), \theta_k)}^{\psi}(\theta_k)\|. \end{aligned}$$

In Eq.(35), let $\theta = \theta_k$, $g_1 = -\hat{g}_k$, $g_2 = -\nabla J(\theta_k)$, $h(x) \equiv 0$, then the following statement holds

$$\mathcal{J}(\theta_{k+1}) \leq \mathcal{J}(\theta_k) - \left(\zeta \alpha_k - \frac{L\alpha_k^2}{2} \right) \|\mathcal{G}_{\alpha_k, \ell(-\hat{g}_k, \theta_k)}^{\psi}(\theta_k)\|^2 + \alpha_k \langle \epsilon_k, \mathcal{G}_{\alpha_k, \ell(-\nabla J(\theta_k), \theta_k)}^{\psi}(\theta_k) \rangle + \frac{\alpha_k}{L} \|\epsilon_k\|^2. \tag{37}$$

Summing the above Eq.(37) from $k = 1$ to N and with the condition $\alpha_k \leq \frac{\zeta}{L}$, we have the following statement

$$\begin{aligned}
\sum_{k=1}^N (\zeta \alpha_k - L \alpha_k^2) \|\mathcal{G}_{\alpha_k, \ell(-\hat{g}_k, \theta_k)}^\psi(\theta_k)\|^2 &\leq \sum_{k=1}^N (\zeta \alpha_k - \frac{L \alpha_k^2}{2}) \|\mathcal{G}_{\alpha_k, \ell(-\hat{g}_k, \theta_k)}^\psi(\theta_k)\|^2 \\
&\leq \sum_{k=1}^N [\alpha_k \langle \epsilon_k, \mathcal{G}_{\alpha_k, \ell(-\nabla J(\theta_k), \theta_k)}^\psi(\theta_k) \rangle + \frac{\alpha_k}{\zeta} \|\epsilon_k\|^2] + \mathcal{J}(\theta_1) - \mathcal{J}(\theta_{k+1}) \\
&\leq \sum_{k=1}^N [\alpha_k \langle \epsilon_k, \mathcal{G}_{\alpha_k, \ell(-\nabla J(\theta_k), \theta_k)}^\psi(\theta_k) \rangle + \frac{\alpha_k}{\zeta} \|\epsilon_k\|^2] + \mathcal{J}(\theta_1) - \mathcal{J}(\theta^*).
\end{aligned} \tag{38}$$

Recall $g_k = \sum_{t=0}^{H_{\tau_k}} \nabla_{\theta} \log \pi_{\theta}(a_t | s_t) R(\tau_k)$, by policy gradient theorem Sutton et al. [2000], we have $\mathbb{E}[-g_k] = -\nabla J(\theta_k) = \nabla \mathcal{J}(\theta_k)$. Let \mathcal{F}_k be the σ -field generated by all random variables defined before round k , $\tilde{\epsilon}_k = g_k - \nabla J(\theta_k)$ then we have: for $k = 1, \dots, N$, $\mathbb{E}[\langle \tilde{\epsilon}_k, \mathcal{G}_{\alpha_k, \ell(-\nabla J(\theta_k), \theta_k)}^\psi(\theta_k) \rangle | \mathcal{F}_{k-1}] = 0$. Let $\delta_s = \sum_{t=1}^s \tilde{\epsilon}_t$, then, for $s = 1, \dots, k$,

$$\mathbb{E}[\langle \delta_s, \tilde{\epsilon}_{s+1} \rangle | \delta_s] = 0. \tag{39}$$

Furthermore, the following statement holds

$$\mathbb{E}[\|\delta_k\|^2] = \mathbb{E}[\|\delta_{k-1}\|^2 + 2\langle \delta_{k-1}, \tilde{\epsilon}_k \rangle + \|\tilde{\epsilon}_k\|^2] \stackrel{(39)}{=} \mathbb{E}[\|\delta_{k-1}\|^2 + \|\tilde{\epsilon}_k\|^2] = \dots = \sum_{t=1}^k \mathbb{E}\|\tilde{\epsilon}_t\|^2. \tag{40}$$

By result (6) and Eq.(40), we have $\mathbb{E}[\|\epsilon_k\|^2] = \frac{1}{k^2} \sum_{t=1}^k \mathbb{E}\|\tilde{\epsilon}_t\|^2 \leq \frac{\sigma^2}{k}$. Combining this result with Eq.(38), and taking expectation w.r.t \mathcal{F}_N , we have

$$\sum_{k=1}^N (\zeta \alpha_k - L \alpha_k^2) \mathbb{E}[\|\mathcal{G}_{\alpha_k, \ell(-\hat{g}_k, \theta_k)}^\psi(\theta_k)\|^2] \leq \mathcal{J}(\theta_1) - \mathcal{J}(\theta^*) + \frac{\sigma^2}{\zeta} \sum_{k=1}^N \frac{\alpha_k}{k}.$$

Now, consider the output $\tilde{\theta}_N = \theta_n$ follows the distribution of Eq.(16), we have

$$\mathbb{E}[\|\mathcal{G}_{\alpha_n, \ell(-g_n, \theta_n)}^\psi(\theta_n)\|^2] \leq \frac{(J(\theta^*) - J(\theta_1)) + \frac{\sigma^2}{\zeta} \sum_{k=1}^N \frac{\alpha_k}{k}}{\sum_{k=1}^N (\zeta \alpha_k - L \alpha_k^2)} =: \frac{\Delta + \frac{\sigma^2}{\zeta} \sum_{k=1}^N \frac{\alpha_k}{k}}{\sum_{k=1}^N (\zeta \alpha_k - L \alpha_k^2)}.$$

□

Remark B.2. Particularly, if the step-size α_k is fixed to a constant: $\zeta/2L$, then

$$\mathbb{E}[\|\mathcal{G}_{\alpha_n, \ell(-\hat{g}_n, \theta_n)}^\psi(\theta_n)\|^2] \leq \frac{4L(J(\theta^*) - J(\theta_1)) + 2\sigma^2 \sum_{k=1}^N \frac{1}{k}}{N\zeta^2}.$$

Recall the following estimation

$$\sum_{k=1}^N \frac{1}{k} = \ln N + C + o(1),$$

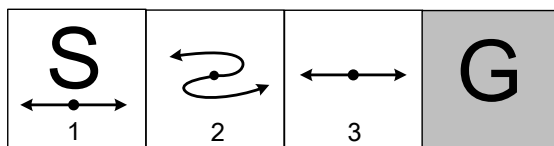
where C is the Euler constant—a positive real number and $o(1)$ is infinitesimal. Thus the overall convergence rate reaches $\mathcal{O}(\frac{\ln N}{N})$ since

$$\mathbb{E}[\|\mathcal{G}_{\alpha_n, \ell(-\hat{g}_n, \theta_n)}^\psi(\theta_n)\|^2] \leq \frac{4LD_J^2 + 2\sigma \sum_{k=1}^N \frac{1}{k}}{N\zeta} = \mathcal{O}(\frac{\ln N}{N}) = \tilde{\mathcal{O}}(\frac{1}{N}),$$

where we use $\tilde{\mathcal{O}}$ to hide polylogarithmic factors in the input parameters, i.e., $\tilde{\mathcal{O}}(f(x)) = \mathcal{O}(f(x) \log(f(x))^{\mathcal{O}(1)})$.

C Appendix B: Short Corridor with Switched Actions (SASC)

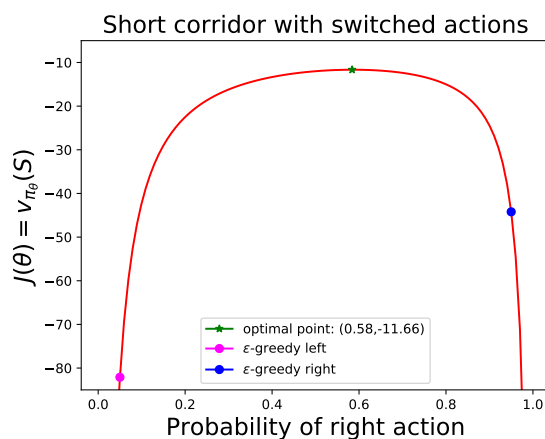
We consider the small corridor grid world which contains three states $\mathcal{S} = \{1, 2, 3\}$. The reward is -1 per step. In each of the three nonterminal states there are only two actions, **right** and **left**. These actions have their usual consequences in the state 1 and state 3 (**left** causes no movement in the first state), but in the state 2 they are reversed, so that **right** moves to the left and **left** moves to the right.



(a)

Figure 4: Short corridor with switched actions (see Chapter 13 of (Sutton and Barto 2018)).

An action-value method with ϵ -greedy action selection is forced to choose between just two policies: choosing **right** with high probability $1 - \frac{\epsilon}{2}$ on all steps or choosing **left** with the same high probability on all time steps. If $\epsilon = 0.1$, then these two policies achieve a value (at the start state) of less than -44 and -82 , respectively, as shown in the following graph.



(a)

Figure 5: The expected return $J(\theta)$ as a function of probability of right action. We plot this figure according to an open source code https://github.com/ShangtongZhang/reinforcement-learning-an-introduction/blob/master/chapter13/short_corridor.py.

A method can do significantly better if it can learn a specific probability with which to select right. The best probability is about 0.58, which achieves a value of about -11.6 .

D Appendix C: Proof of Theorem 4.1

Theorem 4.1 (Convergence Rate of VRMPO) *Consider $\{\tilde{\theta}_k\}_{k=1}^K$ generated by Algorithm 2. Under Assumption 2.1, and let $\zeta > \frac{5}{32}$. For any positive scalar ϵ , let batch size of the trajectories of the outer loop*

$$N_1 = \left(\frac{1}{8L\zeta^2} + \frac{1}{2(\zeta - \frac{5}{32})} \left(1 + \frac{1}{32\zeta^2} \right) \right) \frac{\sigma^2}{\epsilon^2},$$

$$m - 1 = N_2 = \sqrt{\left(\frac{1}{8L\zeta^2} + \frac{1}{2(\zeta - \frac{5}{32})} \left(1 + \frac{1}{32\zeta^2} \right) \right) \frac{\sigma}{\epsilon}},$$

the outer loop times

$$K = \frac{8L(\mathbb{E}[\mathcal{J}(\tilde{\theta}_0)] - \mathcal{J}(\theta^*)) \left(1 + \frac{1}{16\zeta^2} \right)}{\sqrt{\left(\frac{1}{8L\zeta^2} + \frac{1}{2(\zeta - \frac{5}{32})} \left(1 + \frac{1}{32\zeta^2} \right) \right) \left(\zeta - \frac{5}{32} \right)}} \frac{\sigma}{\epsilon},$$

and step size $\alpha = \frac{1}{4L}$. Then, Algorithm 2 outputs $\tilde{\theta}_K$ satisfies

$$\mathbb{E} \left[\|\mathcal{G}_{\alpha, \langle -\nabla J(\tilde{\theta}_K), \theta \rangle}^{\psi}(\tilde{\theta}_K)\| \right] \leq \epsilon. \quad (41)$$

Lemma D.1. *Let $\zeta > \frac{5}{32}$, the batch size of the trajectories of outer loop*

$$N_1 = \frac{\left(\frac{1}{8L\zeta^2} + \frac{1}{2(\zeta - \frac{5}{32})} \left(1 + \frac{1}{32\zeta^2} \right) \right) \sigma^2}{\epsilon^2},$$

the iteration times of inner loop

$$m - 1 = N_2 = \frac{\sqrt{\left(\frac{1}{8L\zeta^2} + \frac{1}{2(\zeta - \frac{5}{32})} \left(1 + \frac{1}{32\zeta^2} \right) \right) \sigma}}{\epsilon},$$

and step size $\alpha_k = \frac{1}{4L}$. For each k and t , $G_{k,0}$ and $\theta_{k,0}$ are generated by Algorithm 2, under Assumption 2.1, then the following holds,

$$\mathbb{E} \|\nabla \mathcal{J}(\theta_{k,0}) - G_{k,0}\|^2 \leq \left(\frac{1}{8L\zeta^2} + \frac{1}{2(\zeta - \frac{5}{32})} \left(1 + \frac{1}{32\zeta^2} \right) \right)^{-1} \epsilon^2. \quad (42)$$

Proof.

$$\mathbb{E}\|\nabla\mathcal{J}(\theta_{k,0}) - G_{k,0}\|^2 = \mathbb{E}\left\|\nabla\mathcal{J}(\theta_{k,0}) - \frac{1}{N_1}\sum_{i=1}^{N_1}g(\tau_i|\theta_{k,0})\right\|^2 \quad (43)$$

$$= \frac{1}{N_1^2}\sum_{i=1}^{N_1}\mathbb{E}\|\nabla\mathcal{J}(\theta_{k,0}) - g(\tau_i|\theta_{k,0})\|^2 \quad (44)$$

$$\stackrel{(6)}{\leq} \frac{\sigma^2}{N_1} = \left(\frac{1}{8L\zeta^2} + \frac{1}{2(\zeta - \frac{5}{32})}\left(1 + \frac{1}{32\zeta^2}\right)\right)^{-1} \epsilon^2. \quad (45)$$

□

To simplify expression, in the following paragraph we use δ denote the long term of (45):

$$\left(\frac{1}{8L\zeta^2} + \frac{1}{2(\zeta - \frac{5}{32})}\left(1 + \frac{1}{32\zeta^2}\right)\right)^{-1} \epsilon^2 \stackrel{\text{def}}{=} \delta^2. \quad (46)$$

D.1 (Proof of Theorem 4.1)

By the definition of Bregman gradient mapping in Eq.(10) and iteration (29), let $\alpha_k = \alpha$, we have

$$\frac{1}{\alpha}(\theta_{k,t} - \theta_{k,t+1}) \stackrel{(29)}{=} \underbrace{\frac{1}{\alpha}\left(\theta_{k,t} - \arg\min_u \left\{\langle G_{k,t}, u \rangle + \frac{1}{\alpha_k}D_\psi(u, \theta_{k,t})\right\}\right)}_{g_{k,t}} \stackrel{(10)}{=} \mathcal{G}_{\alpha, \langle G_{k,t}, u \rangle}^\psi(\theta_{k,t}), \quad (47)$$

where we introduce $g_{k,t}$ to simplify notations.

Step 1: Analyze the inner loop of Algorithm 2

Now, we analyze the inner loop of Algorithm 2. Let $\eta = \frac{\zeta - \frac{5}{32}}{4L}$, our goal is to prove

$$\mathbb{E}[\mathcal{J}(\tilde{\theta}_k)] - \mathbb{E}[\mathcal{J}(\tilde{\theta}_{k-1})] \leq -\sum_{t=1}^{m-1}\left(\eta\mathbb{E}[\|g_{k,t}\|^2] - \frac{\alpha}{2}\epsilon^2\right),$$

In fact,

$$\begin{aligned} \mathcal{J}(\theta_{k,t+1}) &\stackrel{(32)}{\leq} \mathcal{J}(\theta_{k,t}) + \langle \nabla\mathcal{J}(\theta_{k,t}), \theta_{k,t+1} - \theta_{k,t} \rangle + \frac{L}{2}\|\theta_{k,t+1} - \theta_{k,t}\|^2 \\ &\stackrel{(47)}{=} \mathcal{J}(\theta_{k,t}) - \alpha\langle \nabla\mathcal{J}(\theta_{k,t}), g_{k,t} \rangle + \frac{L\alpha^2}{2}\|g_{k,t}\|^2 \\ &= \mathcal{J}(\theta_{k,t}) - \alpha\langle \nabla\mathcal{J}(\theta_{k,t}) - G_{k,t}, g_{k,t} \rangle - \alpha\langle G_{k,t}, g_{k,t} \rangle + \frac{L\alpha^2}{2}\|g_{k,t}\|^2 \\ &\leq \mathcal{J}(\theta_{k,t}) + \frac{\alpha}{2}\|\nabla\mathcal{J}(\theta_{k,t}) - G_{k,t}\|^2 - \alpha\langle G_{k,t}, g_{k,t} \rangle + \left(\frac{L\alpha^2}{2} + \frac{\alpha}{2}\right)\|g_{k,t}\|^2 \end{aligned} \quad (48)$$

$$\stackrel{(34)}{\leq} \mathcal{J}(\theta_{k,t}) + \frac{\alpha}{2}\|\nabla\mathcal{J}(\theta_{k,t}) - G_{k,t}\|^2 - \zeta\alpha\|g_{k,t}\|^2 + \left(\frac{L\alpha^2}{2} + \frac{\alpha}{2}\right)\|g_{k,t}\|^2, \quad (49)$$

Eq.(48) holds due to the Cauchy-Schwarz inequality $|\langle \mathbf{u}, \mathbf{v} \rangle| \leq \|\mathbf{u}\| \|\mathbf{v}\| \leq \frac{1}{2}(\|\mathbf{u}\|^2 + \|\mathbf{v}\|^2)$ for any $\mathbf{u}, \mathbf{v} \in \mathbb{R}^n$. Eq.(49) holds if $h \equiv 0$ by Eq.(34).

Taking expectation on both sides of Eq.(49), we have

$$\begin{aligned} \mathbb{E}[\mathcal{J}(\theta_{k,t+1})] &\leq \mathbb{E}[\mathcal{J}(\theta_{k,t})] + \frac{\alpha}{2} \mathbb{E}[\|\nabla \mathcal{J}(\theta_{k,t}) - G_{k,t}\|^2] - \left(\zeta \alpha - \frac{L\alpha^2}{2} - \frac{\alpha}{2} \right) \mathbb{E}[\|g_{k,t}\|^2] \\ &\leq \mathbb{E}[\mathcal{J}(\theta_{k,t})] + \frac{\alpha}{2} \sum_{i=1}^t \frac{L^2}{N_2} \mathbb{E}\|\theta_{k,i+1} - \theta_{k,i}\|^2 \\ &\quad + \frac{\alpha}{2} \mathbb{E}\|G_{k-1,0} - \nabla \mathcal{J}(\theta_{k-1,0})\|^2 - \left(\zeta \alpha - \frac{L\alpha^2}{2} - \frac{\alpha}{2} \right) \mathbb{E}\|g_{k,t}\|^2 \end{aligned} \quad (50)$$

Eq.(50) holds due to since:

$$\mathbb{E}[\|G_{k,t} - \nabla \mathcal{J}(\theta_{k,t})\|^2] \leq \sum_{i=1}^t \frac{L^2}{N_2} \mathbb{E}[\|\theta_{k,i+1} - \theta_{k,i}\|^2] + \mathbb{E}[\|G_{k-1,0} - \nabla \mathcal{J}(\tilde{\theta}_{k-1})\|^2]. \quad (51)$$

By Lemma D.1, Eq.(50) and Eq.(47), we have

$$\mathbb{E}[\mathcal{J}(\theta_{k,t+1})] \leq \mathbb{E}[\mathcal{J}(\theta_{k,t})] + \frac{\alpha^3 L^2}{2N_2} \sum_{i=1}^t \mathbb{E}[\|g_{k,i}\|^2] + \frac{\alpha \delta^2}{2} - \left(\zeta \alpha - \frac{L\alpha^2}{2} - \frac{\alpha}{2} \right) \mathbb{E}\|g_{k,t}\|^2,$$

where ϵ_1 is defined in (46). Recall the parameter $\tilde{\theta}_{k-1} = \theta_{k-1,m}$ is generated by the last time of

$(k - 1)$ -th episode, now, we consider the following equation

$$\begin{aligned}
& \mathbb{E}[\mathcal{J}(\theta_{k,t+1})] - \mathbb{E}[\mathcal{J}(\tilde{\theta}_{k-1})] \\
& \leq \frac{\alpha^3 L^2}{2N_2} \sum_{j=1}^t \sum_{i=1}^j \mathbb{E}\|g_{k,i}\|^2 + \frac{\alpha}{2} \sum_{j=1}^t \delta^2 - \left(\zeta\alpha - \frac{L\alpha^2}{2} - \frac{\alpha}{2} \right) \sum_{j=1}^t \mathbb{E}\|g_{k,j}\|^2 \\
& \leq \frac{\alpha^3 L^2}{2N_2} \sum_{j=1}^t \sum_{i=1}^t \mathbb{E}\|g_{k,i}\|^2 + \frac{\alpha}{2} \sum_{j=1}^t \delta^2 - \left(\zeta\alpha - \frac{L\alpha^2}{2} - \frac{\alpha}{2} \right) \sum_{j=1}^t \mathbb{E}\|g_{k,j}\|^2 \\
& = \frac{\alpha^3 L^2 t}{2N_2} \sum_{i=1}^t \mathbb{E}\|g_{k,i}\|^2 + \frac{\alpha}{2} \sum_{j=1}^t \delta^2 - \left(\zeta\alpha - \frac{L\alpha^2}{2} - \frac{\alpha}{2} \right) \sum_{j=1}^t \mathbb{E}\|g_{k,j}\|^2 \\
& \leq \frac{\alpha^3 L^2 (m-1)}{2N_2} \sum_{i=1}^t \mathbb{E}\|g_{k,i}\|^2 + \frac{\alpha}{2} \sum_{j=1}^t \delta^2 - \left(\zeta\alpha - \frac{L\alpha^2}{2} - \frac{\alpha}{2} \right) \sum_{j=1}^t \mathbb{E}\|g_{k,j}\|^2 \tag{52} \\
& = \frac{\alpha}{2} \sum_{j=1}^t \delta^2 - \underbrace{\left(\zeta\alpha - \frac{L\alpha^2}{2} - \frac{\alpha}{2} - \frac{\alpha^3 L^2 (m-1)}{2N_2} \right)}_{\stackrel{\text{def}}{=} \eta = \frac{\zeta - \frac{5}{32}}{4L}} \sum_{j=1}^t \mathbb{E}\|g_{k,j}\|^2
\end{aligned}$$

$$= - \sum_{i=1}^t \left(\eta \mathbb{E}[\|g_{k,i}\|^2] - \frac{\alpha}{2} \underbrace{\left(\left(\frac{1}{8L\zeta^2} + \frac{1}{2 \left(\zeta - \frac{5}{32} \right)} \left(1 + \frac{1}{32\zeta^2} \right) \right) \right)^{-1}}_{=\delta^2}} \epsilon^2 \right), \tag{53}$$

Eq.(52) holds due to $t \leq m - 1$.

If $t = m - 1$, then the last Eq.(53) implies

$$\mathbb{E}[\mathcal{J}(\tilde{\theta}_k)] - \mathbb{E}[\mathcal{J}(\tilde{\theta}_{k-1})] \leq - \sum_{t=1}^{m-1} \left(\eta \mathbb{E}[\|g_{k,t}\|^2] - \frac{\alpha}{2} \delta^2 \right). \tag{54}$$

Step 2: Analyze the outer loop of Algorithm 2

We now consider the output of Algorithm 2,

$$\begin{aligned}
\mathbb{E}[\mathcal{J}(\tilde{\theta}_K)] - \mathbb{E}[\mathcal{J}(\tilde{\theta}_0)] &= \left(\mathbb{E}[\mathcal{J}(\tilde{\theta}_1)] - \mathbb{E}[\mathcal{J}(\tilde{\theta}_0)] \right) + \left(\mathbb{E}[\mathcal{J}(\tilde{\theta}_2)] - \mathbb{E}[\mathcal{J}(\tilde{\theta}_1)] \right) \\
&\quad + \cdots + \left(\mathbb{E}[\mathcal{J}(\tilde{\theta}_K)] - \mathbb{E}[\mathcal{J}(\tilde{\theta}_{K-1})] \right) \\
&\stackrel{(54)}{\leq} - \sum_{t=0}^{m-1} \left(\eta \mathbb{E} \|g_{1,t}\|^2 - \frac{\alpha}{2} \delta^2 \right) - \sum_{t=0}^{m-1} \left(\eta \mathbb{E} \|g_{2,t}\|^2 - \frac{\alpha}{2} \delta^2 \right) \\
&\quad - \cdots - \sum_{t=0}^{m-1} \left(\eta \mathbb{E} \|g_{K,t}\|^2 - \frac{\alpha}{2} \delta^2 \right) \\
&= - \sum_{k=1}^K \sum_{t=0}^{m-1} \left(\eta \mathbb{E} \|g_{k,t}\|^2 - \frac{\alpha}{2} \delta^2 \right) \\
&= - \sum_{k=1}^K \sum_{t=1}^{m-1} \left(\eta \mathbb{E} \|g_{k,t}\|^2 \right) + \frac{K\alpha}{2} \delta^2,
\end{aligned}$$

then we have

$$\sum_{k=1}^K \sum_{t=1}^{m-1} \left(\eta \mathbb{E} \|g_{k,t}\|^2 \right) \leq \mathbb{E}[\mathcal{J}(\tilde{\theta}_0)] - \mathcal{J}(\theta^*) + \frac{K(m-1)\alpha}{2} \delta^2. \quad (55)$$

Recall the notation in Eq.(47)

$$g_{k,t} = \frac{1}{\alpha} (\theta_{k,t} - \arg \min_u \{ \langle G_{k,t}, u \rangle + \frac{1}{\alpha} D_\psi(u, \theta_{k,t}) \}) = \mathcal{G}_{\alpha, \langle G_{k,t}, u \rangle}^\psi(\theta_{k,t}),$$

and we introduce following $\tilde{g}(\theta_{k,t})$ to simplify notations,

$$\begin{aligned}
\tilde{g}(\theta_{k,t}) &= \mathcal{G}_{\alpha, \langle -\nabla J(\theta_{k,t}), u \rangle}^\psi(\theta_{k,t}) \stackrel{\text{def}}{=} \tilde{g}_{k,t} \\
&= \frac{1}{\alpha} \left(\theta_{k,t} - \arg \min_u \left\{ \langle -\nabla J(\theta_{k,t}), u \rangle + \frac{1}{\alpha} D_\psi(u, \theta_{k,t}) \right\} \right). \quad (56)
\end{aligned}$$

Then, the following holds

$$\begin{aligned}
\mathbb{E} \|\tilde{g}_{k,t}\|^2 &\leq \mathbb{E} \|g_{k,t}\|^2 + \mathbb{E} \|\tilde{g}_{k,t} - g_{k,t}\|^2 \\
&\stackrel{(35)}{\leq} \mathbb{E} \|g_{k,t}\|^2 + \frac{1}{\zeta^2} \mathbb{E} \|\nabla \mathcal{J}(\theta_{k,t}) - G_{k,t}\|^2, \quad (57)
\end{aligned}$$

Eq.(57) holds due to the Eq.(35).

Let ν be the number that is selected randomly from $\{1, \dots, (m-1)K\}$ which is the output of Algorithm 2, for the convenience of proof there is no harm in hypothesis that $\nu = k \cdot (m-1) + t$ and we denote the output $\theta_\nu = \theta_{k,t}$.

Now, we analyze above Eq.(57) and show it is bounded as following two parts (59) and (62)

$$\mathbb{E} \|g(\theta_\nu)\|^2 = \frac{1}{(m-1)K} \sum_{k=1}^K \sum_{t=1}^{m-1} \mathbb{E} \|g_{k,t}\|^2 \stackrel{(55)}{\leq} \frac{\mathbb{E}[\mathcal{J}(\tilde{\theta}_0)] - \mathcal{J}(\theta^*)}{(m-1)K\eta} + \frac{\alpha}{2\eta} \delta^2, \quad (58)$$

which implies the following holds

$$\mathbb{E}\|g_{k,t}\|^2 \leq \frac{\mathbb{E}[\mathcal{J}(\tilde{\theta}_0)] - \mathcal{J}(\theta^*)}{(m-1)K\eta} + \frac{\alpha}{2\eta}\delta^2. \quad (59)$$

For another part of Eq.(57), notice $\nu = k(m-1) + t$, then we have

$$\mathbb{E}\|\nabla\mathcal{J}(\theta_{k,t}) - G_{k,t}\|^2 = \mathbb{E}\|\nabla\mathcal{J}(\theta_\nu) - G_\nu\|^2 \quad (60)$$

$$\begin{aligned} &\stackrel{(51)}{\leq} \mathbb{E}\left[\frac{L^2}{N_2} \sum_{i=1}^t \mathbb{E}\|\theta_{k,i+1} - \theta_{k,i}\|^2 + \mathbb{E}\|G_{k-1,0} - \nabla\mathcal{J}(\tilde{\theta}_{k-1})\|^2\right] \\ &\stackrel{(42)}{\leq} \mathbb{E}\left[\frac{L^2}{N_2} \sum_{i=1}^t \mathbb{E}\|\theta_{k,i+1} - \theta_{k,i}\|^2 + \frac{\alpha}{2}\delta^2\right] \\ &\stackrel{(47)}{=} \mathbb{E}\left[\frac{L^2\alpha^2}{N_2} \sum_{i=1}^t \mathbb{E}\|g_{k,i}\|^2\right] + \frac{\alpha}{2}\delta^2 \\ &\stackrel{t \leq m}{\leq} \mathbb{E}\left[\frac{L^2\alpha^2}{N_2} \sum_{i=1}^{m-1} \mathbb{E}\|g_{k,i}\|^2\right] + \frac{\alpha}{2}\delta^2 \\ &\leq \frac{L^2\alpha^2}{KN_2} \sum_{k=1}^K \sum_{t=1}^{m-1} \mathbb{E}\|g_{k,t}\|^2 + \frac{\alpha}{2}\delta^2 \end{aligned} \quad (61)$$

$$\stackrel{(55)}{\leq} \frac{L^2\alpha^2}{KN_2\eta} \left(\mathbb{E}[\mathcal{J}(\tilde{\theta}_0)] - \mathcal{J}(\theta^*)\right) + \left(\frac{L^2\alpha^3(m-1)}{2N_2\eta} + \frac{\alpha}{2}\right)\delta^2, \quad (62)$$

Eq.(61) holds due to the fact that the probability of selecting $\nu = k \cdot (m-1) + t$ is less than $\frac{1}{K}$.

Taking Eq(58) and Eq.(61) into Eq.(57), then we have the following inequity

$$\mathbb{E}\|\tilde{g}_{k,t}\|^2 \leq \left(\frac{1}{(m-1)K\eta} + \frac{L^2\alpha^2}{KN_2\eta\zeta^2}\right) \left(\mathbb{E}[\mathcal{J}(\tilde{\theta}_0)] - \mathcal{J}(\theta^*)\right) + \left(\frac{L^2\alpha^3(m-1)}{2N_2\eta\zeta^2} + \frac{\alpha}{2\zeta^2} + \frac{\alpha}{2\eta}\right)\delta^2.$$

Recall $\alpha = \frac{1}{4L}$,

$$N_1 = \frac{\left(\frac{1}{8L\zeta^2} + \frac{1}{2\left(\zeta - \frac{5}{32}\right)} \left(1 + \frac{1}{32\zeta^2}\right)\right) \sigma^2}{\epsilon^2},$$

$$N_2 = m-1 = \frac{\sqrt{\left(\frac{1}{8L\zeta^2} + \frac{1}{2\left(\eta - \frac{5}{32}\right)} \left(1 + \frac{1}{32\zeta^2}\right)\right) \sigma}}{\epsilon},$$

then we have

$$\mathbb{E}\|\mathcal{G}_{\alpha, \langle -\nabla\mathcal{J}(\tilde{\theta}_K), \theta \rangle}\|^2 = \mathbb{E}\|\tilde{g}_{k,t}\|^2 \leq \frac{4L}{K(m-1)\left(\zeta - \frac{5}{32}\right)} \left(1 + \frac{1}{16\zeta^2}\right) \left(\mathbb{E}[\mathcal{J}(\tilde{\theta}_0)] - \mathcal{J}(\theta^*)\right) + \frac{1}{2}\epsilon^2. \quad (63)$$

Furthermore, since

$$K = \frac{8L(1 + \frac{1}{16\zeta^2})}{(m-1)(\zeta - \frac{5}{32})} \cdot \frac{\mathbb{E}[\mathcal{J}(\tilde{\theta}_0)] - \mathcal{J}(\theta^*)}{\epsilon^2} = \frac{8L(\mathbb{E}[\mathcal{J}(\tilde{\theta}_0)] - \mathcal{J}(\theta^*))(1 + \frac{1}{16\zeta^2})}{\sqrt{(\frac{1}{8L\zeta^2} + \frac{1}{2(\zeta - \frac{5}{32})}(1 + \frac{1}{32\zeta^2}))(\zeta - \frac{5}{32})}} \frac{\sigma}{\epsilon},$$

we have

$$\mathbb{E}[\|\mathcal{G}_{\alpha, \langle -\nabla J(\tilde{\theta}_K), \theta \rangle}^{\psi}(\tilde{\theta}_K)\|] \leq \epsilon. \quad (64)$$

E On-line VRMPO

F Experiments

F.1 Additional experiments

We compare the VRMPO with baseline algorithms on test scores and max-return. All the results are shown in Figure 6-7.

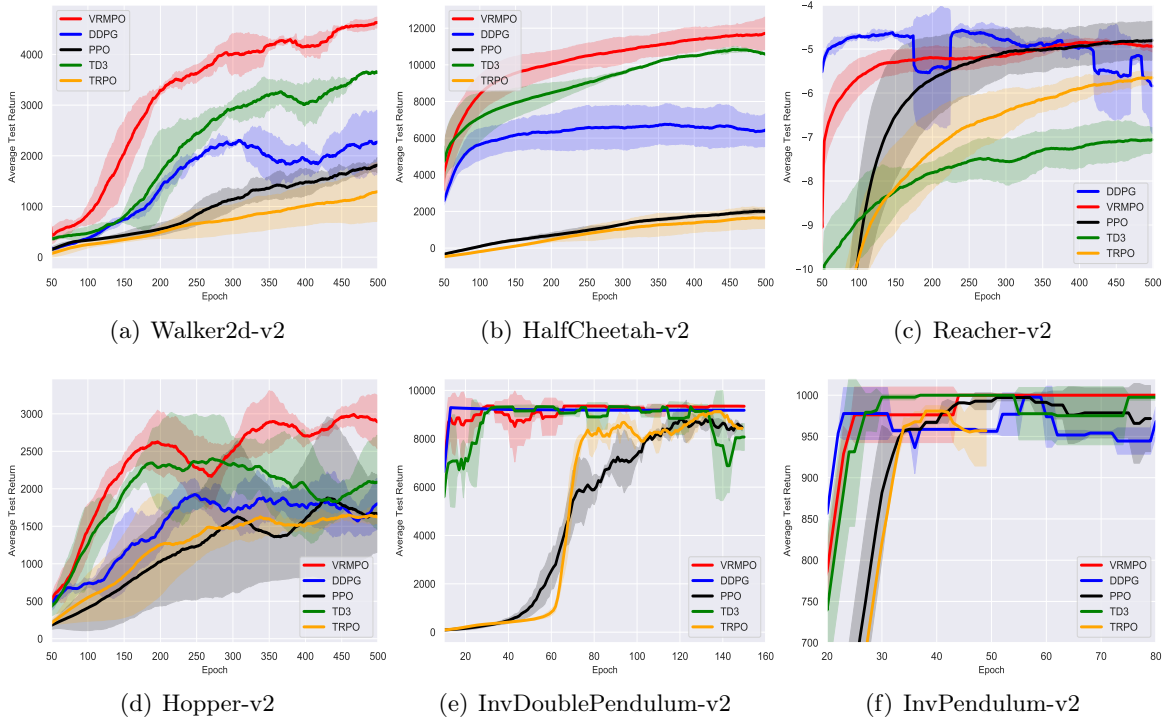


Figure 6: Learning curves of test score over the epoch, where we run 5000 iterations for each epoch. The shaded region represents the standard deviation of the test score over the best 3 trials. Curves are smoothed uniformly for visual clarity.

F.2 E.1: Some Practical Tricks for an On-line Implementation of VRMPO

In this section, we present the details of the practical tricks for an on-line implementation of VRMPO that extends the previous Algorithm 2. We have provided a complete implementation in Algorithm 3.

It is noteworthy that the policy gradient (26) of VRMPO is an off-line (i.e., known as the Monte Carlo method) estimator as the standard REINFORCE. As pointed by Sutton and Barto [2018], REINFORCE converges asymptotically to a local minimum, but like all Monte Carlo methods it tends to learn slowly, to be inconvenient for continuous control tasks, and it is limited in the application to some complex domains. This could also happen in VRMPO. To eliminate above inconveniences and to gain the advantages of VRMPO to complex tasks, we introduce some practical tricks for on-line implementation of VRMPO.

(i) Firstly, we extend Algorithm 2 to be an actor-critic Konda and Tsitsiklis [2000] structure, i.e., we introduce a critic structure to Algorithm 2. Concretely, for each step t , we construct a critic network (an estimator of action-value) $Q_\omega(s, a)$ with the parameter ω , sample $\{(s_i, a_i)\}_{i=1}^N$ from a

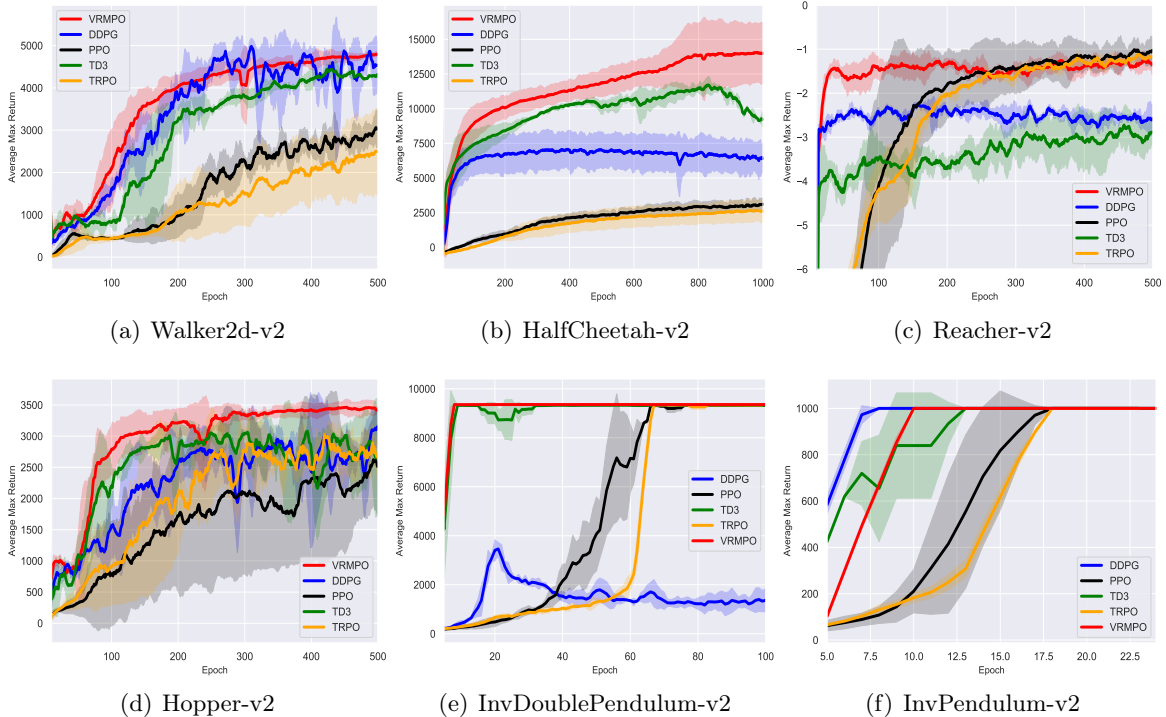


Figure 7: Learning curves of max-return over the epoch, where we run 5000 iterations for each epoch. The shaded region represents the standard deviation of the test score over the best 3 trials. Curves are smoothed uniformly for visual clarity.

data memory \mathcal{D} , and learn the parameter ω via minimizing the following fundamental critic loss:

$$L_{\omega} = \frac{1}{N} \sum_{i=1}^N (Q_{\omega_{k-1}}(s_i, a_i) - Q_{\omega}(s_i, a_i))^2. \quad (70)$$

For the complex real-world domains, we should tune necessitate meticulous hyper-parameter. In order to improve sample efficiency, we draw on the technique of **Double Q-learning** Van Hasselt et al. [2016] to VRMPO. For more details, please see **Line 17-20** of Algorithm 3.

For the implementation of critic network $Q_{\omega}(s, a)$, we use a two-layer feedforward neural network of 400 and 300 hidden nodes respectively, with rectified linear units (ReLU) between each layer, and a final tanh unit following the output of the critic network $Q_{\omega}(s, a)$. After coding the critic network $Q_{\omega}(s, a)$, we get the loss of critic L_{ω} (70)/(68), we use adaptive strategies to compute the step-size according to **ADaptive Moment estimation (ADAM)** Kingma and Ba [2015] to learning the parameter ω . Concretely, for (69), we use Tensorflow to return the parameter ω : `tf.train.AdamOptimizer(learning_rate = 1r).minimize($L_{\omega_{k-1, t-1}^j}(\omega)$)`, where the step-size `1r` is chosen by grid search from the set $\{0.1, 0.01, 0.004, 0.008\}$.

(ii) Let \mathcal{D} be the replay memory, in this section, we set the memory size $|\mathcal{D}| = 10^6$. For each pair $(s, a) \sim \mathcal{D}$, we conduct the following actor loss

$$L_{\theta}(s, a) = -\log \pi_{\theta}(s, a) \underbrace{\left(\min_{j=1,2} Q_{\omega_{k-1}^j}(s, a) \right)}_{\text{Double Q-Learning Van Hasselt et al. [2016]}} \quad (71)$$

to replace $J(\theta)$. Then, we calculate the “noise” gradient $\frac{1}{N_2} \sum_{j=1}^{N_2} (-g(\tau_j|\theta_{k,t}) + g(\tau_j|\theta_{k,t-1}))$ as the following $\delta_{k,t}$

$$\delta_{k,t} = \frac{1}{N_2} \sum_{i=1}^{N_2} (\nabla_{\theta} L_{\theta_{k,t}}(s_i, a_i) - \nabla_{\theta} L_{\theta_{k,t-1}}(s_i, a_i)), \quad (72)$$

where $\{(s_i, a_i)\}_{i=1}^{N_2} \sim \mathcal{D}$. For more details, please see **Line 13-16** of Algorithm 3.

For the implementation of policy π , we use a Gaussian estimator as follows,

$$\pi_{\theta}(a|s) = \frac{1}{\sigma_{\theta} \sqrt{2\pi}} \exp\left(-\frac{a - \mu_{\theta}(s)}{2\sigma_{\theta}^2}\right),$$

where the logarithmic standard deviation estimator $\log \sigma_{\theta}$ as follows, we use a two layer feedforward neural network of 400 and 300 hidden nodes respectively, with rectified linear units (ReLU) between each layer, and a final tanh unit produces a scalar `net_output_value`; then we use

$$\log \sigma_{\theta} = \text{LOG_STD_MIN} + \frac{1}{2}(\text{LOG_STD_MAX} - \text{LOG_STD_MIN})(\text{net_output_value} + 1),$$

where `LOG_STD_MIN` = -20 and `LOG_STD_MAX` = 2. $\mu_{\theta}(s) = \text{action_space.high}[0] * \text{net_output_value}$, which makes sure actions are in correct range. In this step, we use $\alpha_k = 0.2$ for the iteration (67) and the mirror map ψ is ℓ_2 -norm.

F.3 E.2. Details of Implementation of Baseline Algorithms

In this section, we provide all the details of implementation of baseline algorithms. All algorithms, we set $\gamma = 0.99$. For VRMPO, the learning rate is chosen by grid search from the set $\{0.1, 0.01, 0.004, 0.008\}$, batch-size $N = 100$. Memory size $|\mathcal{D}| = 10^6$. We run 5000 iterations for each epoch.

DDPG For the implementation of DDPG, we also use a two-layer feedforward neural network of 400 and 300 hidden nodes, respectively, with rectified linear units (ReLU) between each layer for both the actor architecture and critic architecture, and a final tanh unit following the output of the actor. The step-size of the actor architecture is 10^{-3} , step-size of the critic architecture is 10^{-1} , and batch size is 10^2 .

In this experiment of DDPG, we set the number of steps of interaction (state-action pairs) for the agent and the environment in each epoch to be 5000. The replay size is 10^6 . To help exploration, we store enough data to train a model in the replay, and the starting time of training is 10000. $\gamma = 0.99$, the maximum episode is 1000. Both target network are updated with soft update $\kappa = 0.005$

TD3 For our implementation of TD3, we refer to the work Fujimoto et al. [2018] and <https://github.com/sfujim/TD3>.

We excerpt some necessary details about the implementation of TD3 Fujimoto et al. [2018]. TD3 maintains a pair of critics along with a single actor. For each time step, we update the pair of critics towards the minimum target value of actions selected by the target policy:

$$y = r + \gamma \min_{i=1,2} Q_{\theta'_i}(s', \pi_{\phi'}(s') + \epsilon),$$

$$\epsilon \sim \text{clip}(\mathcal{N}(0, \sigma), -c, c).$$

Every d iterations, the policy is updated with respect to Q_{θ_1} following the deterministic policy gradient algorithm. The target policy smoothing is implemented by adding $\epsilon \sim \mathcal{N}(0, 0.2)$ to the actions chosen by the target actor network, clipped to $(-0.5, 0.5)$, delayed policy updates consists of only updating the actor and target critic network every d iterations, with $d = 2$. While a larger d would result in a larger benefit with respect to accumulating errors, for a fair comparison, the critics are only trained once per time step, and training the actor for too few iterations would cripple learning. Both target networks are updated with $\tau = 0.005$.

TRPO For implementation of TRPO, we refer an open source <https://spinningup.openai.com/en/latest/algorithms/trpo.html>. Recall the basic problem of TRPO as follows,

$$\theta_{k+1} = \arg \max_{\theta} \mathcal{L}(\theta_k, \theta), \quad \text{s.t. } D_{\text{KL}}(\pi_{\theta} | \pi_{\theta_k}) \leq \delta, \quad (73)$$

where where $\mathcal{L}(\theta_k, \theta)$ is the surrogate advantage, a measure of how policy π_{θ} performs relative to the old policy π_{θ_k} using data from the old policy: $\mathcal{L}(\theta_k, \theta) = \mathbb{E}_{(s,a) \sim \pi_{\theta_k}} \left[\frac{\pi_{\theta}(a|s)}{\pi_{\theta_k}(a|s)} A^{\pi_{\theta_k}} \right]$, $A^{\pi_{\theta_k}}$ is the advantage function estimator, and $D_{\text{KL}}(\pi_{\theta} | \pi_{\theta_k})$ is Kullback-Leibler (KL) divergence. Usually, to get an answer of (73) quickly, according to Schulman et al. [2015], we consider the following problem to approximate the original problem (73),

$$\theta_{k+1} = \arg \max_{\theta} g^{\top} (\theta - \theta_k) \quad \text{s.t. } \frac{1}{2} (\theta - \theta_k)^{\top} H (\theta - \theta_k) \leq \delta, \quad (74)$$

where g is a policy estimator, H is the Hessian matrix with respect to $\mathcal{L}(\theta_k, \theta)$. TRPO adds a modification to this update rule: a backtracking line search,

$$\theta_{k+1} = \theta_k + \alpha^j \sqrt{\frac{2\delta}{g^{\top} H^{-1} g}} H^{-1} g,$$

where $\alpha \in (0, 1)$ is the backtracking coefficient, and j is the smallest nonnegative integer such that $\pi_{\theta_{k+1}}$ satisfies the KL constraint and produces a positive surrogate advantage.

For the experiments, we run the parameter δ in the set $\{10^{-2}, 2 \times 10^{-2}, 4 \times 10^{-2}, 8 \times 10^{-2}\}$. We set $\gamma = 0.995$ and the maximum episode to be 1000. For the implementation of critic network, we use a two-layer feedforward neural network of 64 and 64 hidden nodes, respectively, with tanh activation between each layer, and the learning rate of critic network is 10^{-3} . The actor is also Gaussian policy as same as our VRMPO in Appendix F.2 and the learning rate of critic network is 10^{-2} . We use ADAM to learn both actor network and critic network. For each each epoch, we let the agent interact with the environment up to be 5×10^3 . We run the backtracking coefficient in the set in the set $\{10^{-1}, 2 \times 10^{-1}, 4 \times 10^{-1}, 8 \times 10^{-1}\}$.

PPO. For the implementation of PPO, we refer to an open source <https://github.com/openai/baselines/tree/master/baselines>.

PPO develops TRPO, and its objective reduces to

$$L(s, a, \theta_k, \theta) = \min \left\{ \frac{\pi_{\theta}(a|s)}{\pi_{\theta_k}(a|s)} A^{\pi_{\theta_k}}(s, a), g(\epsilon, A^{\pi_{\theta_k}}(s, a)) \right\},$$

where $g(\epsilon, A) = (1 + \epsilon)A$, if $A \geq 0$; else, $g(\epsilon, A) = (1 - \epsilon)A$. In this experiment, we use the same actor-critic network as TRPO, and clip parameter $\epsilon = 0.2$.